Since January 2020 Elsevier has created a COVID-19 resource centre with free information in English and Mandarin on the novel coronavirus COVID-19. The COVID-19 resource centre is hosted on Elsevier Connect, the company's public news and information website.

Chemical Engineering Journal 416 (2021) 129071

Contents lists available at ScienceDirect

Chemical Engineering Journal

journal homepage: www.elsevier.com/locate/cej

Antimicrobial TiO_2 nanocomposite coatings for surfaces, dental and orthopaedic implants

Vignesh Kumaravel [a,b,*], Keerthi M. Nair [a,b,1], Snehamol Mathew [a,b,1], John Bartlett [a,b], James E. Kennedy [c], Hugh G. Manning [c], Barry J. Whelan [c], Nigel S. Leyland [c], Suresh C. Pillai [a,b,*]

[a] Nanotechnology and Bio-Engineering Research Group, Department of Environmental Science, School of Science, Institute of Technology Sligo, Ash Lane, Sligo, Ireland
[b] Centre for Precision Engineering, Materials and Manufacturing Research (PEM), Institute of Technology Sligo, Ash Lane, Sligo, Ireland
[c] Kastus Technologies, Cookstown, Dublin, Ireland

ARTICLE INFO

Keywords:
Photocatalyst
SARS-CoV-2
MRSA
E. coli
Biofilm
ROS

ABSTRACT

Engineering of self-disinfecting surfaces to constrain the spread of SARS-CoV-2 is a challenging task for the scientific community because the human coronavirus spreads through respiratory droplets. Titania (TiO_2) nanocomposite antimicrobial coatings is one of the ideal remedies to disinfect pathogens (virus, bacteria, fungi) from common surfaces under light illumination. The photocatalytic disinfection efficiency of recent TiO_2 nanocomposite antimicrobial coatings for surfaces, dental and orthopaedic implants are emphasized in this review. Mostly, inorganic metals (*e.g.* copper (Cu), silver (Ag), manganese (Mn), *etc*), non-metals (*e.g.* fluorine (F), calcium (Ca), phosphorus (P)) and two-dimensional materials (*e.g.* MXenes, MOF, graphdiyne) were incorporated with TiO_2 to regulate the charge transfer mechanism, surface porosity, crystallinity, and the microbial disinfection efficiency. The antimicrobial activity of TiO_2 coatings was evaluated against the most crucial pathogenic microbes such as *Escherichia coli,* methicillin-resistant *Staphylococcus aureus*, *Pseudomonas aeruginosa*, *Bacillus subtilis, Legionella pneumophila, Staphylococcus aureus, Streptococcus mutans,* T2 bacteriophage, H1N1, HCoV-NL63, vesicular stomatitis virus, bovine coronavirus. Silane functionalizing agents and polymers were used to coat the titanium (Ti) metal implants to introduce superhydrophobic features to avoid microbial adhesion. TiO_2 nanocomposite coatings in dental and orthopaedic metal implants disclosed exceptional bio-corrosion resistance, durability, biocompatibility, bone-formation capability, and long-term antimicrobial efficiency. Moreover, the commercial trend, techno-economics, challenges, and prospects of antimicrobial nanocomposite coatings are also discussed briefly.

1. Introduction

The outbreak of various infectious diseases such as SARS-CoV, H1N1, and Ebola has resulted in a significant impact on the global economy and health systems [1,2]. SARS-CoV-2 is the most recent pandemic, caused by the human coronavirus [3–5]. The global mortality rate of SARS-CoV-2 is increasing everyday owing to its extremely contagious characteristics. At this stage, the world is fighting against an invisible enemy to control rampant infections and save lives. Studies are in progress on various aspects such as rapid detection, development of vaccines, medication, therapy, *etc* [6–8]. There is an urgent need to develop self-disinfecting surfaces to control the spread of this disease. Photocatalytic surface coatings would be considered one of the best solutions to disinfect pathogens from the most commonly touched surfaces, such as commercial touch screens, mobile phones, ceramics, *etc* [9,10]. Non-toxic metal oxides are commonly used for photocatalytic coatings, which could respond to light and moisture to generate the reactive oxygen species (ROSs), to destroy the microbes. Compared to normal sanitation procedures, durable photocatalytic coatings could hinder the reactivation of microbes and destroy them completely. The mobility of ROSs in the air is normally higher and so it could effectively destroy airborne microbes [1]. Titanium dioxide or titania (TiO_2) is one of the best photocatalysts for commercial antimicrobial coatings owing to its low-cost, reactivity, stability, reusability, durability, biocompatibility,

* Corresponding authors.
E-mail addresses: Kumaravel.Vignesh@itsligo.ie (V. Kumaravel), Pillai.Suresh@itsligo.ie (S.C. Pillai).
[1] These authors contributed equally.

https://doi.org/10.1016/j.cej.2021.129071
Received 14 December 2020; Received in revised form 13 February 2021; Accepted 16 February 2021
Available online 23 February 2021

crystallinity, high surface area and corrosion resistance. Very recently, the inactivation of a human coronavirus (HCoV-NL63) using TiO_2 nanoparticles coated glass coverslips has been studied in various humid environments under UV radiation [11]. In another study, the photocatalytic activity of TiO_2 coated films has been investigated against the bovine coronavirus under visible light irradiation of 500 lx [12]. Sandia National Laboratory, USA also reported the efficacy of Ag-TiO_2 coated surfaces against the vesicular stomatitis virus (the biosafety level-2 safe surrogate virus for SARS-CoV-2) under visible light irradiation [13]. All these recent studies clearly suggest that TiO_2 coatings are effective to disinfect the coronavirus and the related viral genomic RNA. The photocatalytic disinfection mechanism of coronavirus on a TiO_2 coated mobile phone touch screen through the attack of ROSs is schematically illustrated in Fig. 1.

TiO_2 coated surfaces could minimise microbial adhesion by altering the surface free energy [14]. TiO_2 is one of the broad-spectrum bactericides with self-sterilizing effects and it could reduce the number of adhered microbes through increasing the electron donor surface energy of the coating [15–18]. In most of the recent studies, TiO_2 has been doped with metals/non-metals or other chemical modifiers to extend the light absorption into the visible region and improve the photo-generated charge-transfer process [19–22].

Imani *et al.* reported the effectivity of inorganic (such as copper (Cu), silver (Ag), zinc (Zn), silica, *etc.*) and organic (such as polyethylenimine, porphyrin, quaternary ammonium compounds, C_{60}, *etc.*) coatings to prevent the spread of viral infections through contaminated surfaces [23]. Nevertheless, the bare metal or polymer coatings could fail to deliver long-term antimicrobial efficiency and could be easily corroded under certain circumstances [14,24–26]. Environmentally benign TiO_2 photocatalytic coatings with active ingredients are one of the best options to address the long-term antimicrobial efficiency with anti-corrosion surface features. There are no comprehensive reviews on the applications of TiO_2 nanocomposite photocatalytic coatings for antimicrobial applications. Coatings of TiO_2 with active inorganic metals/organic polymers/2D materials could demonstrate the maximum microbial disinfection efficacy compared to bare metals or TiO_2 [23]. This review focuses on the application of various TiO_2 nanocomposite antimicrobial coatings for surfaces and medical (dental and orthopaedic) implants.

2. Principles and mechanism

Biofilm formation, proliferation, and the efficacy of ROSs on the microbes are briefly discussed in this section. The surface interaction of microbes is crucial as they establish alterations in the gene expression of cells, which influences the behaviour, morphology and surface adhesion of the cells [27]. Understanding these mechanisms can guide the engineering of novel materials or technologies to inhibit microbial growth and proliferation.

2.1. Biofilm formation

Bacteria are unicellular organisms, but in nature they are attached to inert or active surfaces to form well-structured three-dimensional (3D) communities known as 'biofilms' [28]. Biofilms can be formed from either a single or multiple species and they can protect the microbes from antibiotic treatments and stress conditions. The cycle of biofilm formation can be generally described through 5 steps (Fig. 2). Step 1: In response to a specific environmental signal in a free-living cell, they attach to the surface using Van der Walls force and form an organic monolayer of polysaccharides or glycol proteins. Step 2: Once the biofilm layer is formed, the cells move along using twitching motility that involves the extinction of a specific pilin monomer (PilA). This could facilitate an irreversible cell attachment to the surface. Step 3: Microcolonies are formed once more cells are attached to the surface. When the biofilm matures, it communicates between the colonies by sending and receiving autoinducer signals (AI), this communication is called quorum sensing (QS) [29]. QS is favourable to promote the development of biofilms into a 3D structure. Step 4: In response to environmental changes, there can be metabolic features and genetic expressions of the cell. They tend to uptake foreign DNA and result in expressing exogenous proteins. This step supports the cells in adapting to the surrounding conditions, such as the formation of antibiotic-resistant strains. Once it reaches a specific concentration, the genetic changes in the cells will be triggered, which causes the cells to bind to a substrate and each other. Step 5: This stage is called dispersion, the matured sessile cells are released by shedding the biofilm and moving to new places, forming other colonies by repeating this cycle [28].

Photo-generated ROSs exhibited hormone effects on the biofilm formation [30]. The changing trends of AI (such as c-di-GMP) and QS signals (such as AHL and AI-2) during the development of biofilm stages could be disturbed by the ROSs attack [30]. The processes (suppress the production of AI, degradation of AI, inhibition of AI binding to the respective receptors, and prevention of biofilm gene expression and transcription) involved in the inactivation of QS signals (called quorum quenching) is shown in Fig. S1 [31]. The key steps of QS and the communication between the colonies in biofilm could be blocked by the photocatalytic coatings.

2.2. Photocatalytic mechanism

A schematic of ROSs formation through semiconductor photocatalysis is displayed in Fig. 3. The primary ROSs formed at the photocatalyst surface are hydroxyl radical ($^{\bullet}OH$), singlet oxygen ($^1O_2$), superoxide radical ($O_2^{\bullet-}$), and hydrogen peroxide (H_2O_2) [32,33]. Amongst these ROSs, $O_2^{\bullet-}$ and H_2O_2 are formed by the reduction of O_2, which then further dissociates to form $^{\bullet}OH$ [34]. The anatase and rutile phases of TiO_2 have distinct reactivity towards $^{\bullet}OH$ and $O_2^{\bullet-}$ formation [35]. It could be ascribed to the differences in their adsorption towards

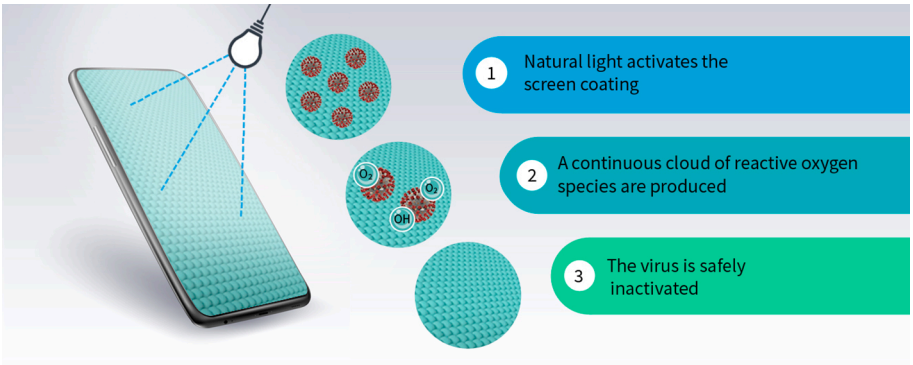

Fig. 1. Schematic of photocatalytic disinfection mechanism on a mobile phone screen.

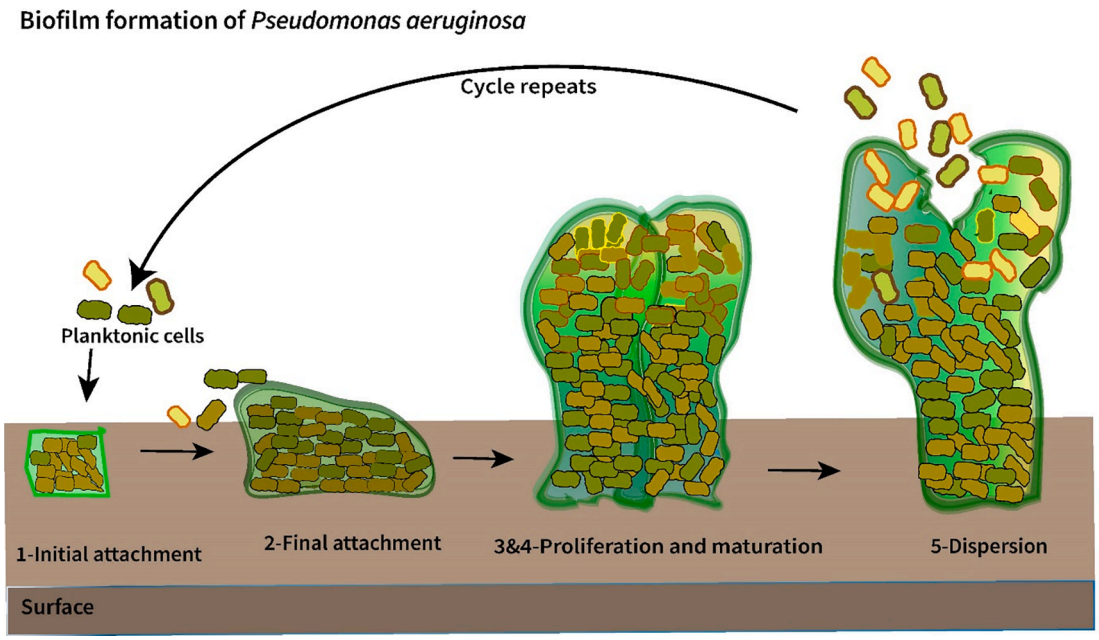

Fig. 2. Schematic of biofilm formation cycles on a surface.

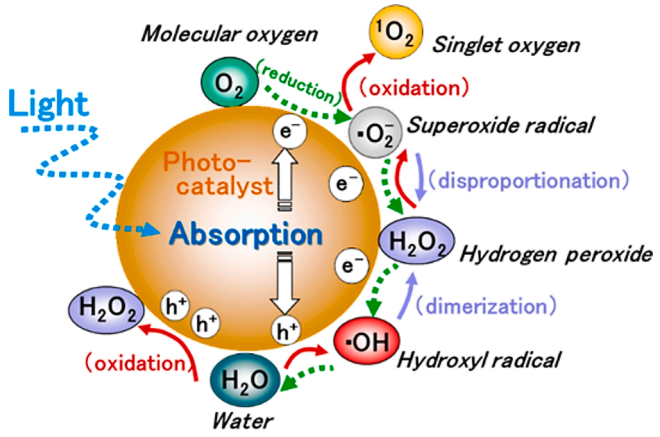

Fig. 3. Schematic of ROSs formation during semiconductor photocatalysis [39]. Reproduced with permission from [39]. Copyrights (2017), American Chemical Society.

H_2O_2 and the alignment of band edges. The lifetime of ROSs in the TiO_2 anatase phase is longer than that of rutile [36]. Compared to the individual polymorphs of TiO_2, a mixture of anatase and rutile phases showed the maximum photocatalytic activity. This could be attributed to the heterojunction formation through the close contact of valance and conduction band edges [37]. ROSs could damage the cells, affect the microbial growth and migration of cells either by direct interaction with the cell membrane or diffusion of H_2O_2 into the cells [38].

2.3. Destruction of biofilm

The attack of ROSs on Gram-positive and Gram-negative bacteria is schematically illustrated in Fig. 4 [40]. The attack of ROSs on the cytoplasm is the most significant mechanism to influence the metabolism, enzymatic, respiratory, and defence process of the microbe. However, the peptidoglycan (PGN) layers are the main barriers for the ROSs before entering the cytoplasmic membrane. Lipopolysaccharides and lipid layers of Gram-negative bacteria could be easily destroyed through the photocatalysis mechanism. PGN layer of Gram-positive bacteria is much thicker and more resistant to the ROSs. Nevertheless, the ROSs could be easily diffused through the pores in the PGN layers without PGN degradation. Once the ROSs reach the cytoplasmic membrane, they could easily affect the key enzymatic and respiratory activities of microbes.

Recently, the activity of TiO_2 on *Pseudomonas aeruginosa* (*P. aeruginosa*) biofilm formation was investigated under UVA irradiation [41]. The effect of ROSs attack in the enzyme lipase, protein expression and biofilm formation were analysed. The rod-shaped morphology of the cells was faded with respect to the irradiation time, suggesting the degradation of cells. After 60 min of treatment, there was a drastic increase in the number of damaged cells (Log 4 reduction), as the viability of bacterial cells was greatly reduced due to the ROSs attack. Furthermore, the motility of planktonic cells was also reduced, this could avoid further colony formation. Under extreme stress environments, the bacteria undergo resistant strategies like viable but non-culturable (VBNC) state to increase the tolerance to ROSs attack and to maintain intact membrane and genetic material. Under photocatalytic reaction, *P. aeruginosa* in planktonic form lost the ability to form a biofilm, as well as undergo disruption of the bacterial cell membrane. For the cells already under biofilm production, the rigidity of the ε-poly (L-lysine) became weak, thus affecting the cell stability. Thus, the photocatalytic treatment of cells with TiO_2 could reduce the bacterial cell density including VBNC and inhibit the biofilm formation.

ROS attack is the principal mechanism for the destruction of biofilms under light illumination of TiO_2. Nevertheless, the electrostatic interaction of the coating materials with the microbial cell wall could cause the leakage of intracellular contents under dark conditions [42]. Moreover, the key metabolic processes, ATP production, and protein synthesis could be inhibited by the interaction of metal ions in the photocatalytic coating with the amino acids of the microbes [43].

2.4. Photocatalytic disinfection of bacteria, and virus

Scanning electron microscopy (SEM) and transmission electron microscopy (TEM) are commonly employed to investigate the changes in cell morphology and the destruction of cell integrity during the microbial disinfection process [44,45].

Bacteria: The photocatalytic disinfection mechanism of bacteria is shown in Fig. 5(a) [46]. At first, the shape of the cell becomes abnormal

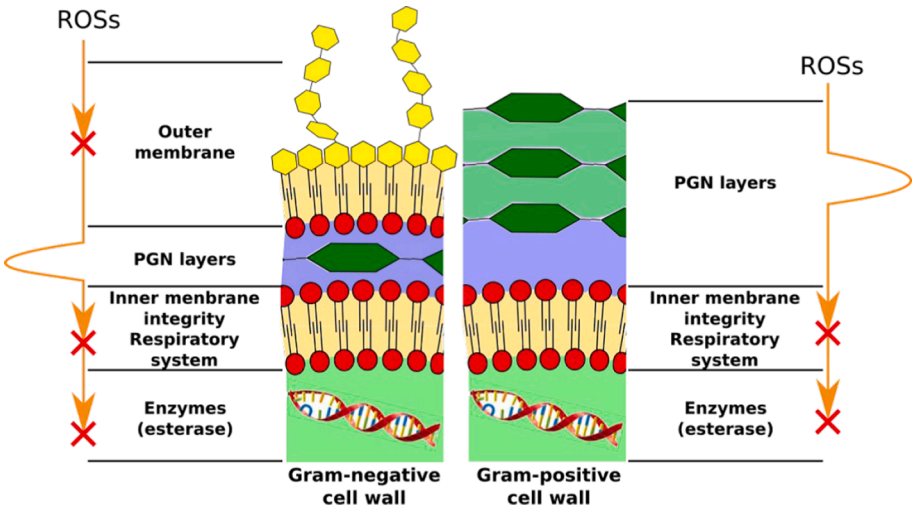

Fig. 4. Schematic of ROSs attack on the Gram-positive and Gram-negative bacteria cell wall [40]. Reproduced with permission from ref. [40]. Copyrights (2020), American Chemical Society.

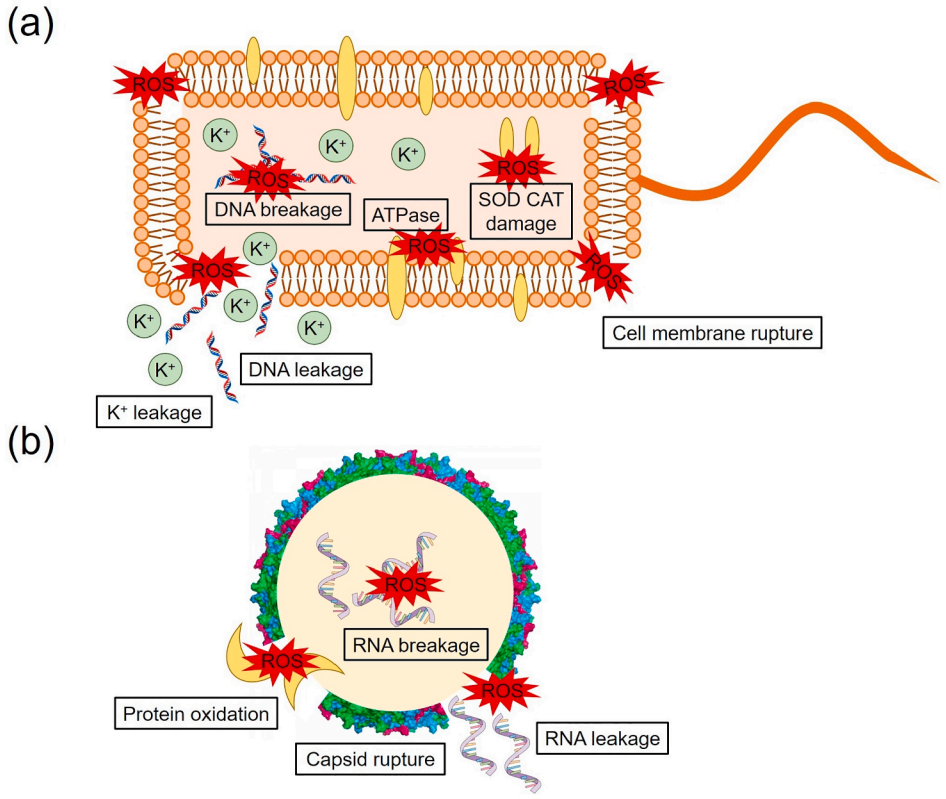

Fig. 5. Photocatalytic disinfection mechanism of (a) bacteria, and (b) virus [46]. Reproduced with permission from ref. [46]. Copyrights (2019), Elsevier.

and then the cell membrane is damaged by the attack of ROSs. This could facilitate the entry of ROSs into the interior of the cells. Afterwards, the cells could be ruptured into small fragments during the prolonged light irradiation [47]. Potassium (K^+) is one of the key elements for the synthesis of proteins and polysomes inside the cells. K^+ ions are released during the cell membrane rupture and therefore cell permeability is commonly analysed through the detection of K^+ concentration [48,49]. The concentrations of key elements such as adenosine triphosphate (ATP, vital for the bacteria metabolism), and antioxidant enzymes (superoxide dismutase (SOD) and catalase (CAT)) could also be reduced through the repetitive attack of ROSs. The bacteria could potentially repair and regrow through self-defence mechanisms [50]. However, the repair or regrowth of cells is not viable, as the leakage or damage of genome DNA/cytoplasm is severe during the constant photocatalytic treatment.

Viruses: The photocatalytic disinfection mechanism of viruses is shown in Fig. 5(b) [46]. Viruses do not have any cell membrane, cytoplasm, and energy metabolism. Consequently, the photocatalytic disinfection of viruses is usually examined *via* analysing the damage of major building blocks such as nucleic acids and proteins. ROSs could interact with the outer layer of surface proteins, which leads to the oxidation of the protein layer and the leakage of enveloped RNA [51]. The important

protein side chains such as threonine, lysine, and arginine could be oxidized by the ROSs attack [52,53]. Electrophoresis is used to explore the decline or disappearance of protein band intensities during the photocatalytic treatment.

2.5. Influence of environmental factors

The photocatalytic activity of TiO_2 under a real-life scenario was tested to provide a basic understanding on the durability of coatings [54]. 1 wt% TiO_2 (42% anatase, and 38% rutile) was dispersed in water and coated on the limestone surfaces. The coatings were exposed in a real urban site for one year. The photocatalytic experiments were carried out for coated and uncoated limestone surfaces before and after light exposure (UV irradiance varied from 6.7 W/m^2 to 27 W/m^2). It was found that the photocatalytic efficiency was reduced by 20% after the second term of exposure and was reduced to almost negligible after one year. Additionally, the surface colour of limestone, which was retained by the TiO_2 coating was also lost by the end of the term of exposure. These results revealed the enormous influence of environmental factors on the stability of photocatalytic coatings. Factors such as humidity, temperature, and concentration of pollutants in the microstructure of the coating could influence the photocatalytic activity of TiO_2. The decrease in efficiency of the coating could be attributed to the blocking of active sites by the degradation intermediates or products. The presence of a higher concentration of Cl^-, which could act as the oxidising radical scavenger in the environment was an additional factor for this adverse effect. However, by washing the coated surface with water, the photocatalytic activity was regained up to 85%. The increase in humidity of the environment reduces the photocatalytic efficiency as the water molecule tends to occupy the active site on the surface rather than the pollutant. This enables the coatings to exhibit a hydrophilic surface effect instead of an oxidising effect. Furthermore, at low temperatures, the photocatalytic activity was reduced, while at increased temperatures the activity was regained as the TiO_2 sites were available due to evaporation of adsorbed water molecules. The deficiency of nanoparticles from the coating surface was also confirmed by X-ray fluorescence (XRF) analysis, where the existence of Ti was reduced over the period. These results suggest that the influence of environmental factors on the activity of TiO_2 must be addressed for the sustainability of coatings in real-life applications [55–57].

3. Recent advances

The development of efficient strategies against microbial infections, both *in-vitro and in-vivo*, is still quite challenging. Although TiO_2 antimicrobial surfaces are widely employed in various sectors, the rapid recombination of the generated holes and electrons limits its practical applications. Strategies such as loading of antibiotics, metal nanoparticles, and other 2D materials could lead to improved microbial disinfection *via* an enhanced ROSs generation. Recent advances on the antimicrobial activity of TiO_2 for the surfaces and medical implants are highlighted in this section. The key findings of TiO_2 nanocomposites for the disinfection of various microbes are given in Table S1.

Sol-gel and hydrothermal techniques are commonly utilised for the synthesis of TiO_2 nanocomposites. The general flow chart for the fabrication of TiO_2 films and nanoparticles is shown in Fig. S2. Numerous methods such as deposition (*e.g.*, spray/dip/spin coating), sputtering, functionalization, and implantation (*e.g.*, electrospinning, electrodeposition, MAO, physical/chemical vapour deposition, and layer by layer assembly) could be used to coat the antimicrobial nanocomposites.

3.1. TiO_2 nanocomposites for surface coatings

Recently, the *in-situ* anti-biofilm activity of phosphorus (P) and fluorine (F) doped TiO_2 coatings were investigated in three microbes, *Escherichia coli (E. coli, SCC1), Staphylococcus epidermidis (S. epidermidis, ATCC 35983),* and *Pseudomonas fluorescens (P. fluorescens, ATCC 13525)* under UVA light irradiation [40]. The influence of P/F-TiO_2 coating on the intracellular enzymatic functions and the respiratory process of the microbes were also examined through fluorescence staining. P/F-TiO_2 was synthesised *via* a sol–gel method, and the molar ratio of F/Ti and P/Ti was fixed at 0.03. To prepare the coatings, the required quantity of P/F-TiO_2 powders was dispersed in ethanol under ultrasonication. The photocatalytic suspension was then drop-casted on a 22 × 22 mm glass substrate with a surface coating density of 1 mg/cm^2. The live and dead microbial population was assessed using a confocal laser scanning microscope (CLSM) after the light irradiation. The efficiency of the P/F-TiO_2 coated glass substrate was also compared with the commercial TiO_2 P25. Fluorescence microscopy images (before and after light illumination), and the surface fraction coverage of live/damaged cells are displayed in Fig. S3. Experiments were also performed in the absence of light or catalyst to demonstrate the impact of the antimicrobial photocatalysis mechanism. Almost all the *E. coli* were destroyed on P/F-TiO_2 coated glass after 10 min treatment. In the case of commercial TiO_2 P25 coated glass, only 50% microbial reduction was measured during 10 min treatment. After 45 min of treatment, the average damaged to live *E. coli* ratio for P/F-TiO_2 and TiO_2 P25 was 1.15 (with an 80% reduction in the enzymatic process) and 0.84 (with a 60% reduction in the enzymatic process), respectively.

The physico-chemical properties of P/F-TiO_2 were superior (such as isoelectric point (3.4 ± 0.2), average particle size (10 nm), high specific surface area (130 m^2/g)) than that of the commercial photocatalyst Degussa (Evonik) P25 TiO_2 (5.6 ± 0.5, 22 nm, and 55 m^2/g). Atomic force microscopy (AFM) results revealed that P/F-TiO_2 coated surface was smoother with small grain sizes (42 ± 16 nm). TiO_2 P25 coated surface was comprised of a huge grain-like morphology with large particle sizes (180 ± 35 nm). Topography results showed that the number of contact points for the microbial adhesion in P/F-TiO_2 was higher than that of TiO_2 P25. Therefore, the ROSs formed in P/F-TiO_2 coated surface could easily enter the microbial cell wall. The long-term efficiency of the light irradiated photocatalyst surface was assessed to examine the survival of microbes under favourable growth conditions for 16 h. Bacterial regrowth was restricted to ~60% by the photocatalyst coated surface. The rate of microbial inactivation for P/F-TiO_2 coated surface was in the following order: *E. coli* > *S. epidermidis* > *P. fluorescens*.

The difference in antimicrobial activity was mainly ascribed to a discrepancy in the surface characteristics (*e.g.*, electrostatic interaction, pH, topology, *etc.*) of the microbe and the coating material. Moreover, anti-oxidant enzymes such as CAT and SOD are available in the three microbes. The ability of anti-oxidative enzymes to defend against the ROSs may vary with respect to the bacterial species [58]. Anaerobic microbes (*E. coli* and *S. epidermidis*) are more sensitive towards O_2 exposure compared to aerobic *P. fluorescens* [59]. Aerobic *P. fluorescens* strains could survive under ROSs attack through generating NADPH, ATP and glyoxylate [60]. The influence of O_2 on the photocatalytic inactivation of *E. coli* was tested. The results revealed that efficiency was reduced under poor O_2 conditions, and that the colour of the coatings changed from white to blue. This was ascribed to the formation of reduced TiO_2 (Ti^{3+}) with O_2 vacancies [61,62]. In the poor O_2 conditions, the photo-generated electrons could accumulate in the TiO_2 and thus reduce the Ti^{4+} species into Ti^{3+}.

A potential three-in-one antimicrobial platform was developed on a gallium (Ga)-carbenicillin (Car) framework coated with oxygen-deficient hollow TiO_2 nano-shells (H-TiO_{2-x}@MOF) to fight against methicillin-resistant *Staphylococcus aureus* (MRSA) and *Pseudomonas aeruginosa* (PA) under visible light irradiation [21]. The oxygen vacancies have proved to narrow the bandgap of TiO_2, improving its optical absorption range towards visible and near-infrared (IR) regions. Antibacterial properties were studied through *in-vitro* and *in-vivo* wound healing. *In-vitro* studies showed that H-TiO_{2-x}@MOF exhibited a higher

antibacterial efficacy towards both MRSA and PA at pH 5.5 compared to that of pH 7.4. This could be attributed to the gradual degradation of Ga-MOF at low external pH similar to the wound microenvironment [63]. The antimicrobial experiments were also carried out under dark conditions. The results showed that the bacterial viability on the coatings with light irradiation was lower than the dark samples, indicating the visible light-driven ROSs generation. The schematic of wound healing experiments is shown in Fig. 6 (A). *In-vivo* healing assays on mice wounds demonstrated that H-TiO_{2-x}@MOF showed a significant reduction in the wound area compared to all other groups (control, Car, Ga, H-TiO_{2-x}, H-TiO_{2-x} + Car, and H-TiO_{2-x} + Ga) (Fig. 6(B), and (D)). The average survival rate of the mice was almost 100% for H-TiO_{2-x}@MOF, whereas the control group only showed a rate below 50% after 14 days (Fig. 6(C)). Histological analysis showed that H-TiO_{2-x}@MOF assisted in re-epithelialization and thickened epidermis in the infected areas and it was completely repaired by the 14th day (Fig. 6(E)). The antimicrobial efficiency of H-TiO_{2-x}@MOF was higher as compared to other samples (Fig. 6(F)). The improved performance of H-TiO_{2-x}@MOF could be attributed to the following features: (i) the abundant oxygen vacancies in H-TiO_{2-x} could increase the yield of ROSs under visible and near IR radiations, (ii) the 'Trojan Horse' strategy of Ga, where Ga^{3+} could incorporate into Fe^{3+} binding bacterial enzymes/proteins synthesis, disrupting the bacterial antioxidation system [64,65], and (iii) the antibacterial effect of Car against PA. In addition, the rough spiky surface of H-TiO_{2-x} could improve the adhesion of bacteria and on-site ROSs generation.

Studies have also shown the significance of nanostructures in upgrading ROSs generation and antimicrobial efficiency. The effect of optical and geometrical parameters on the photocatalytic efficiency of TiO_2 were comprehensively studied by Sen and co-workers [66]. A silicon surface with nanostructured grass-like pillars known as black-silicon was coated on the TiO_2 *via* atomic layer deposition (AT_B-Si) [67–69]. The commonly accepted "contact killing" mechanism and the significance of pillar structures over flat surfaces (AT_Si) on ROSs generation were further investigated [70,71]. The reflection of the incident light, photogeneration of charge carriers, and the electron-hole recombination process on TiO_2 are schematically displayed in Fig. 7(a). The charge carriers are usually generated beyond the first 15 nm but the light diffusion path length for TiO_2 anatase is less than 5 nm, indicating only <5% of photogenerated charge carriers could reach the catalyst surface. Therefore, 99.5% of incident photons could not produce the ROSs in a planar TiO_2 surface. The stepwise processes such as (i) generation of charge carriers *via* interaction of light at sub-wavelength nanopillars, (ii) diffusion of charge carriers inside the nanopillars to produce ROSs, and (iii) diffusion of ROSs out of the nanopillars for the contact killing of microbes are schematically shown in Fig. 7(c). ROSs generated in the bulk of the catalyst might not be effective for the photocatalytic disinfection process. The interaction of light on TiO_2 coated nanopillars with high and low molar extinction coefficients is schematically illustrated in Fig. 7(d) (TiO_2 coated on Si), and (e) (TiO_2 coated on SiO_2 or polydimethoxysiloxane (PDMS)), respectively. The simulations of light-nanopillar interaction on TiO_2–Si and TiO_2 coated on SiO_2 are displayed in the insets of Fig. 7(d) and (e), respectively. Finite-difference time-domain (FDTD) simulations revealed that the total light absorption was 1.8 times higher for TiO_2-Si compared to TiO_2-SiO_2. In the case of TiO_2 – Si, a considerable amount of light was absorbed in the bulk, whereas the light was disseminated inside the TiO_2 – SiO_2 nanopillars to enhance the ROSs generation and photocatalytic activity.

TiO_2-SiO_2 nanopillars exhibited 73% bactericidal efficiency (*E. coli* ATCC 25922) compared to TiO_2-Si. *In-vitro* studies revealed that AT_B-Si caused the bacteria to lose their smoothness by both oxidative stress and an increased ROSs production disrupting the cell wall integrity. Finite element method (FEM) simulations indicated that with an increase in the height of the nanopillars, the absorption on the TiO_2 surface was also increased. However, there is a particular diffusion length associated with the ROSs beyond which the absorption does not lead to an increased ROSs generation. It was concluded that after 5 μm of pillar height, there was no further ROSs production even though the absorption of light increases. This work illustrated a basic design rule for optically activated nanostructured photocatalysts with an improved ROSs generation and antibacterial efficacy.

A specialized reusable filter surface with photocatalytic TiO_2 nanowires (TiO_2NWs) was developed to inactive the airborne pathogens [1]. TiO_2NWs offered an improved photocatalytic efficiency owing to the high surface to volume ratio for ROSs generation [72]. The schematic of ROSs generation on TiO_2NWs filter is displayed in Fig. 8.

The pore size of TiO_2NWs could be easily tuned to allow the efficient trapping of pathogens, including small viruses. Besides, TiO_2NWs offer a high dielectric constant which enhances the electrostatic precipitation of the water droplets on the filter surface. The superhydrophilicity of TiO_2NWs favours the adhesion and spread of the droplets, which could be attributed to the presence of several Ti^{3+} sites on the surface [73–75]. Moisture or humid conditions are essential for the maximum ROSs generation under light illumination. The efficiency of TiO_2NWs was tested using *E. coli*. The bacterial suspension was dropped on the nanofilters which were further exposed to UV illumination for time intervals of 30, 60, 100 and 200 s. SEM images of the *E. coli* suspension after light illumination indicated that most of the bacteria were inactivated at the initial exposure of 30 s. Electrophoresis experiments showed that the DNA treated with TiO_2NWs under UV light irradiation did not reveal any bands indicating the complete degradation of DNA strands. The fragmentation of DNA bands was not observed for the control experiments at dark conditions. Electron spin resonance (ESR) studies were conducted to identify the ROSs generation. 4-hydroxy-2,2,6,6-tetramethylpi-peridine-1-oxyl (called TEMPOL) was used in ESR to target $^{\bullet}OH$ and $O_2^{\bullet-}$ radicals. After 120 min, TEMPOL was completely decayed and a small peak of 4-oxo-TEMPO was observed in the presence of TiO_2NWs under UV exposure, indicating the generation of both $^{\bullet}OH$ and $O_2^{\bullet-}$. The different timescales for ESR and antibacterial studies could be attributed to the importance of a mutual distance between TiO_2NWs and the species in contact. Moreover, TiO_2NWs could be reused more than 1000 times, which could further address the environmental pollution caused by disposable masks.

In a recent study, a hybrid of monolayer MXene ($Ti_3C_2T_x$) incorporated TiO_2 with (001) facets was investigated for the inactivation of airborne microbes [2]. Theoretical and experimental studies reveal that the (001) facet of TiO_2 is more reactive and stable owing to its high surface energy [76]. Besides, the photocatalytic activity of anatase TiO_2 with exposing (001) facets is exceptional to that of commercial P25 [77]. The hybridisation of (001)TiO_2 with monolayer $Ti_3C_2T_x$ two-dimensional (2D) nanosheets could further upgrade the photocatalytic activity through an improved electron-hole separation [78,79]. (001) TiO_2/$Ti_3C_2T_x$ was synthesized with various weight percentages (0.9, 3.4, and 7.2%) of $Ti_3C_2T_x$. Then, the photocatalyst was coated onto a polyurethane (PU) foam and the antimicrobial experiments were carried out in a continuous flow-through reactor under UV light irradiation (356 nm and 254 nm).

The microbial inactivation was studied in *E. coli, Bacillus subtilis (B. subtilis)* and its spore (bacteria in a dormant state). The microbial bioaerosol was produced using an aerosol generator with a particle size of ~1–5 μm. The average particle size of (001)TiO_2/$Ti_3C_2T_x$ was 20–30 nm, and the lattice spacing of (001) facet was ~0.23 nm. UV–visible light absorption intensities of bare TiO_2 and (001)TiO_2/$Ti_3C_2T_x$ samples were almost identical. Compared to bare TiO_2 (3.2 eV), the band gap energy of (001)TiO_2/$Ti_3C_2T_x$ was slightly increased (3.5 ~ 3.65 eV). Nonetheless, the PL intensity of (001)TiO_2/$Ti_3C_2T_x$ was lower than that of bare TiO_2, suggesting that an increased electron-hole separation was achieved on the hybrid catalyst surface. *E. coli* inactivation efficiency was in the following order (Fig. S4(a)): PU foam with UV < photolysis (UV-365 nm alone) < photolysis (UV-254 nm alone) < (001)TiO_2/$Ti_3C_2T_x$ on PU foam at 365 nm < (001)TiO_2/$Ti_3C_2T_x$ on PU foam at 254 nm. The microbial disinfection was not observed on the coatings at dark

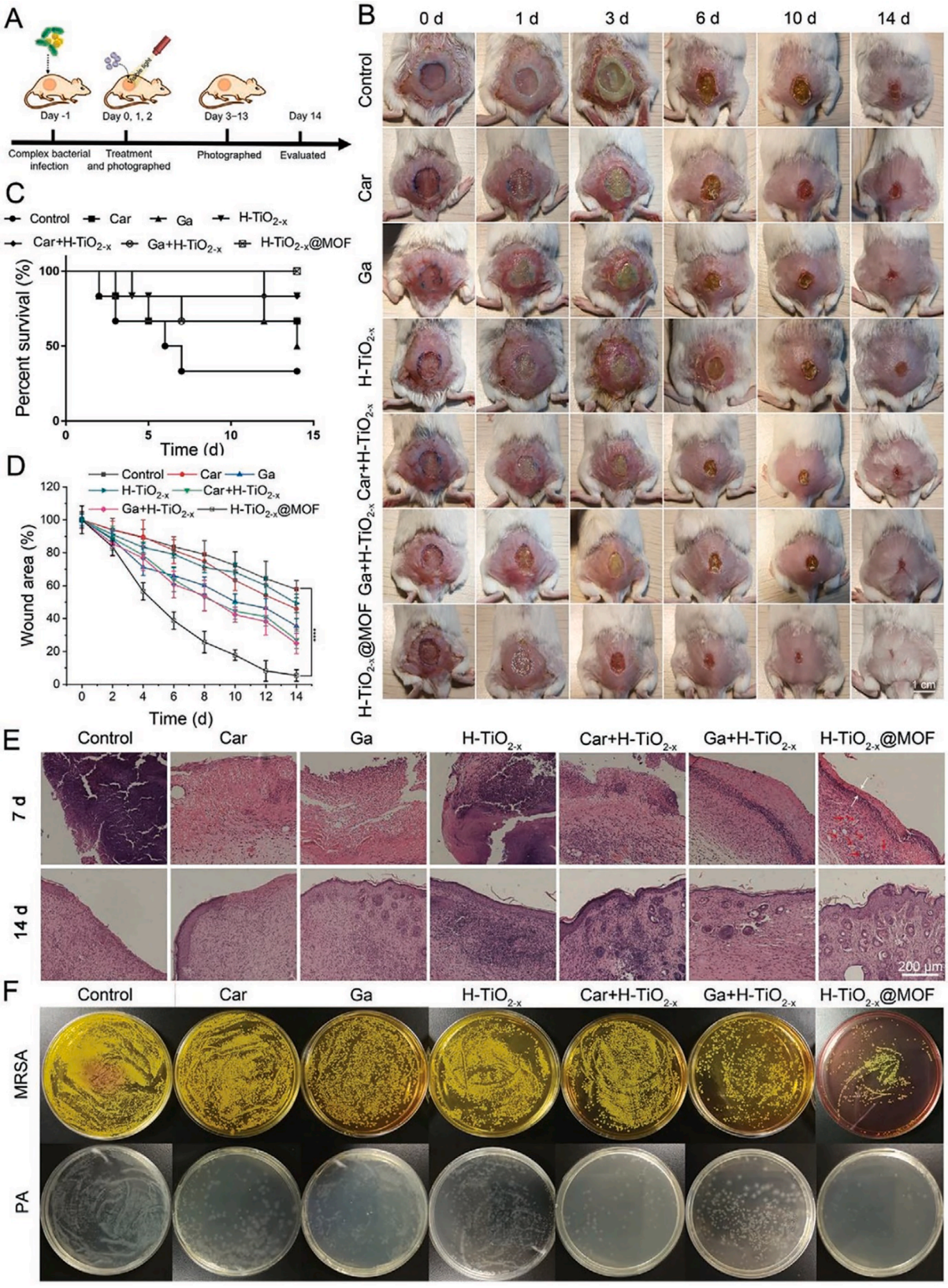

Fig. 6. *In-vivo* studies of wound healing using various materials (Car, Ga, H-TiO_{2-x}@MOF): (A) schematic of the experimental procedure, (B) photographs of the infected wounds at various time intervals, (C) survival rates for 14 days treatment, (D) quantitative representation of the infection percentage at various time intervals, (E) H and E stained images of the tissue sections at 7 and 14 days, and (F) photographs of plated bacterial colonies from the infected skin tissues [21]. Reproduced with permission from [21]. Copyrights (2020), John Wiley and Sons.

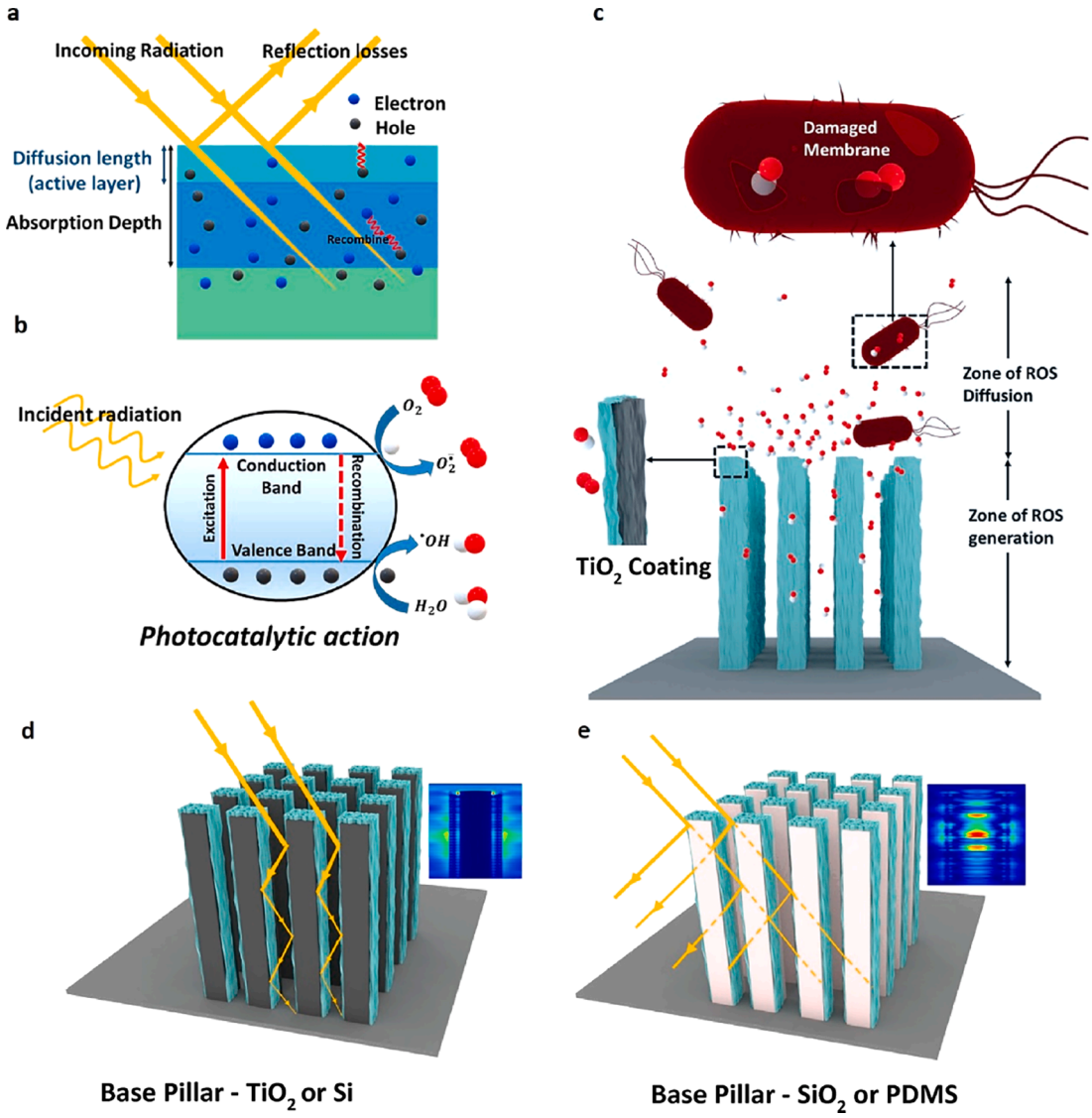

Fig. 7. Schematics: (a) the reflection of incident light, photogeneration of charge carriers, and the electron-hole recombination process on TiO_2, (b) photocatalytic generation of ROSs, (c) stepwise processes for the diffusion of ROSs out of the nanopillars for the contact killing of microbes, (d) interaction of light on TiO_2 coated on Si nanopillars (inset simulations of light-nanopillar interaction), (e) interaction of light on TiO_2 coated on SiO_2 nanopillars [66]. Reproduced with permission from [66]. Copyrights (2020), American Chemical Society.

conditions (Fig. S4(a)). The hybrid photocatalyst with 3.4% of $Ti_3C_2T_x$ showed the highest antimicrobial efficiency compared to others.

Electrical efficiency (EE) per Log order of microbial inactivation was studied to investigate the electricity consumption during photocatalysis and photolysis (Fig. S4(b)). Compared to various metal-doped TiO_2 photocatalysts (Cu-TiO_2, Ag-TiO_2, TiO_2 P25, MOF, *etc*) and UV photolysis, the electricity consumption for (0 0 1)TiO_2/$Ti_3C_2T_x$ on PU foam under UV light irradiation was much smaller. In the case of different microbial species, the photocatalytic efficiency of (0 0 1)TiO_2/$Ti_3C_2T_x$ was in the following order: *E. coli* > *B. subtilis* > spore of *B. subtilis*. DFT studies showed that electron-hole separation and the charge transfer process of the catalyst were upgraded through the high metallic conductivity of MXenes. Moreover, the utilisation of a continuous flow-through reactor could increase the contact area and reduce the retention time. The cell membrane of Gram-positive bacteria is denser with a thick pepti-gosaccharide layer of 20–80 nm, whereas that of Gram-negative bacteria is thinner with a loose pepti-gosaccharide layer of ~10 nm. Consequently, the cell membrane of *B. subtilis* and its spore could protect them from the attack of ROSs during photocatalysis. The Log inactivation efficiency of the photocatalyst was increased with respect to the humidity from 30 to 95%, indicating that the high humid conditions stimulate the photo-generation of ROSs [80,81]. The reactivation of microbes was tested after the treatment of photolysis and photocatalysis. The reactivation of microbes was not observed for the photocatalysis condition whereas the reactivation was noted for dark and photolysis conditions. Bacteria were inactivated through the damage of DNA in the photolysis condition which could be repaired under certain cases. Microbes could enter the VBNC state in response to the light irradiation treatment [82]. However, the photocatalytic microbial inactivation was achieved *via* physical damage of the outer cell membrane by ROSs attack [83]. The microbe could not repair its membrane after the photocatalysis without sufficient nutrition.

In another study, a ternary nanocomposite (TiO_2/SiO_2/Ag) coating was developed for medical devices using a magnetron co-sputtering technique [84]. Mesoporous SiO_2 was used as a seed layer for the homogeneous immobilization of Ag nanoparticles on TiO_2 [85,86]. *E. coli* (ATCC 10536) was selected to evaluate the antimicrobial activity because it is one of the common microbes for urinary tract infection in medical devices [87]. The nanocomposite was coated on glass substrates with various concentrations (9.7, 14.4 and 19.8 at %) of Ag. The

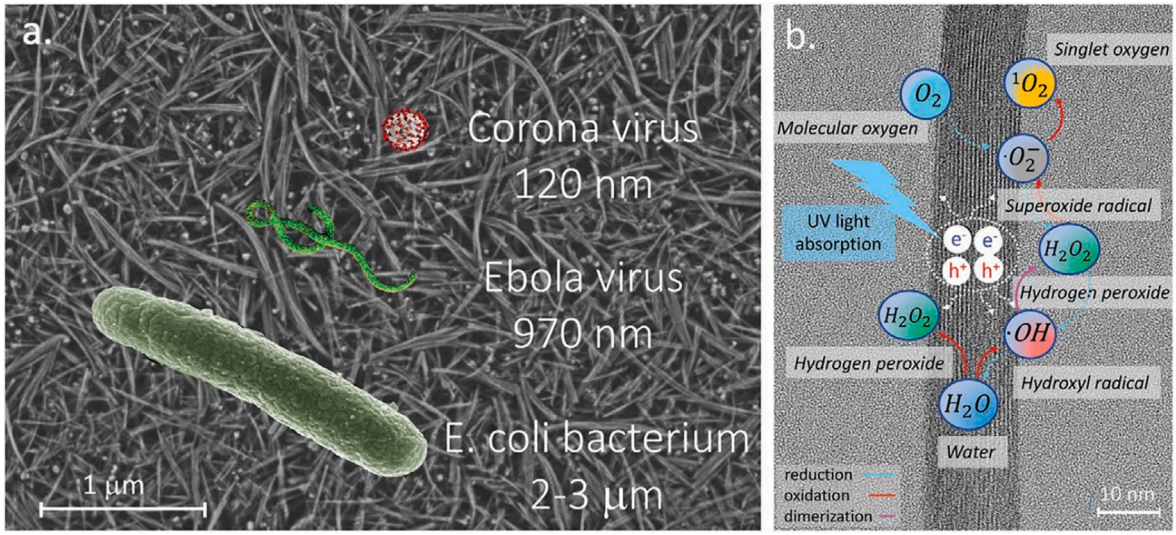

Fig. 8. (a) SEM image of TiO_2NWs filter overlapped with schematic images of pathogens, (b) photocatalytic mechanism of ROSs generation on the humid TiO_2NWs [1]. Reproduced with permission from [1]. Copyrights (2020), John Wiley and Sons.

bacterial growth on the coated substrates was assessed by the most probable number of living cells (MPN) method. WCA of TiO_2/SiO_2, $TiO_2/SiO_2/Ag_{9.7\ at.\ \%}$, $TiO_2/SiO_2/Ag_{14.4\ at.\ \%}$, and $TiO_2/SiO_2/Ag_{19.8\ at.\ \%}$ was 50 ± 0.50, 53.3 ± 0.61, 62.6 ± 0.53, and $70.2 \pm 0.50^{\circ}$, respectively. The hydrophilicity of the coatings was decreased after the deposition of Ag. The surface morphology of the coatings was smoother with a uniform distribution of nanoparticles. MPN results suggested that $TiO_2/SiO_2/Ag$ coatings showed complete *E. coli* inactivation within 2 h compared to control (substrate without coating) and TiO_2/SiO_2. The nanocomposite coatings also showed remarkable antimicrobial activity against *Pseudomonas aeruginosa* (ATCC 12633). The antimicrobial activity was mainly ascribed to the effect of Ag deposition rather than the surface wettability, free energy, and topography. Flame atomic absorption spectroscopy was applied to examine the release of Ag ions from the coatings. The lethal concentration of Ag for the *E. coli* inactivation was estimated as $\sim 6.9 \times 10^{-7}$ mg/cell.

In vivo biofilm formation on coatings under urine flow was evaluated using artificial urine medium (AUM) under simulated urinary tract conditions. Silicone was also tested as a substrate in this study because it is widely used in urinary catheters and stents [88]. Compared to the bare glass, $TiO_2/SiO_2/Ag$ coated substrates showed an outstanding efficiency to inhibit the biofilm formation under the simulated urine flow conditions after 24 and 48 h. The antimicrobial efficiency of the coatings was ascribed to cell membrane damage, leakage of cellular components, changes in cell shape/size, and an increase of cell surface roughness [89]. Also, the Ag nanoparticles were able to bind the microbial proteins to inactive the electron transport chain, inhibit the respiratory process and growth of the cells [90,91].

In recent decades, TiO_2 photocatalysis has also been proven to be effective against viruses [92]. The key findings of recent antiviral TiO_2 nanocomposite coatings are shown in Table S2. The human influenza virus strain of A/PR8/H1N1 was treated with TiO_2 under UV light irradiation, and the efficiency of the viral disinfection process relied on the intensity of the light radiation [93]. Later, a photocatalytic air cleanser was developed using a TiO_2-coated aluminium plate system [94]. It showed maximum efficiency against aerosol-associated influenza virus, indicating the competence of photocatalysis technology to detoxify the indoor air. LED light-driven TiO_2/β-SiC solid alveolar photocatalytic foams were developed for the disinfection of T2 bacteriophage [95]. The overall antiviral efficiency of this nanocomposite was associated with the passive filtration effect of the foams. Further, Cu-TiO_2 nanofibers were designed to inactivate the bacteriophage f2 as well as *E. coli* 285, where the free ROSs in the bulk phase of the photocatalyst played a significant role in the virus inactivation process [96]. Recently, various studies have also been conducted to inactivate the SARS-CoV-2 virus using TiO_2 nanocomposite coatings [12]. TiO_2-Ag coatings with an anatase phase of TiO_2 was engineered through an ion-assisted deposition technique [13]. The exposure of UV light over 9 h showed the complete elimination of SARS-CoV-2 compared to the dark conditions. TiO_2 nanoparticles also displayed high efficiency against the human coronavirus type NL63. The cell infectivity assay demonstrated that the virus strains were disinfected within one minute of UV exposure [11]. Although TiO_2 holds several advantages such as non-toxic, highly economical, and chemical stability, utilization of more sustainable resources including visible/solar light for microbial disinfection is highly desirable in the future [97]. More selective viral inactivation techniques, especially towards the disinfection of SARS-CoV-2 should be further established.

3.2. TiO_2 nanocomposite coatings for medical implants

Ti metal implants are commonly employed in dentistry (*e.g.*, dental implants, dentures) and orthopaedics (*e.g.*, artificial bone, plates, joints, screws, *etc.*) owing to its outstanding bio-corrosion resistance, mechanical strength, and biocompatibility [98–100]. Globally, more than 200 million people are using orthopaedic metal implants for various bone-related diseases [101,102]. However, the biomaterial centred infection (BCI) and the lack of bioactive/antimicrobial ingredients are the most common rationales for implant failures in several patients [103,104]. BCI is usually instigated through the formation, adhesion, and proliferation of biofilm on the implants. Antibiotic treatments are generally recommended to alleviate minor infections after implant surgery. However, the dead cells on the implant surfaces from this bactericidal effect could act as binding sites for other live pathogens [105]. In some cases, the wound healing might be delayed by antibiotic-resistant biofilm formation on the implant. The infected tissue should be replaced through another surgery if the BCI is acute. BCI related implant failures could prolong hospitalisation and cause a considerable economic burden to patients. Consequently, Ti implants with self-disinfection features have been most sought-after in the biomedical industry and clinical medicine. These kinds of implants could prevent postoperative infections, provide long-term antimicrobial efficiency, and promote the binding of implants with the bone tissue.

In a recent study, a two-step micro-arc oxidation (MAO) technique was used to fabricate the TiO_2 nanotubes coating loaded with bioactive (calcium (Ca), phosphorus (P)) and antimicrobial (Ag) materials [106].

The antimicrobial property of Ca-P-Ag/TiO_2 coating was investigated against *Staphylococcus aureus* (ATCC 6538) by the plate count method. MAO could introduce porous features on the Ti implant surface to enhance its adhesion and growth of osteoblasts [106]. At first, Ag-doped TiO_2 nanotubes were fabricated on the Ti surface by anodic oxidation under UV light treatment. Then, the as-synthesized Ag/TiO_2 nanotubes were subjected to MAO oxidation for 10 min in a solution containing Ag, Ca, and P precursors. SEM images of bare and Ag/TiO_2 coated nanotubes are shown in Fig. S5. Nanotubes were formed with a diameter of 100–150 nm and ~20 tubes were noted in 4 μm × 3 μm area (Fig. S5(a)). Spherical shaped Ag particles were attached to the TiO_2 nanotube orifice after 3 h of UV treatment (Fig. S5(b)). After the MAO treatment, the Ca-P-Ag/TiO_2 coating was gully shaped with micro-holes and nanopores on the surface. The spherical shaped Ag particles were evenly distributed, and the surface smoothness of the coating was increased with respect to the MAO voltage (from 320 V to 380 V). The Ag content of Ca-P-Ag/TiO_2 at 380 V was lower than the same at 320 and 350 V. This was attributed to the intense oxidation reaction of Ag at high voltages. At the same time, the Ca and P contents of Ca-P-Ag/TiO_2 were increased as the MAO voltage was increased from 320 (~5 wt% of Ca and P) to 380 V (~10 wt % of Ca and P). The molar ratio of Ca/P at 350 V was ~1.77, which was closer to the Ca/P ratio in bioactive hydroxyapatite (~1.67). Moreover, the microporous surface features of the coating were also maintained well at 350 V.

The growth of *Staphylococcus aureus* at different incubation times on the coating is shown in Fig. S6. The antimicrobial efficiency of Ca-P-Ag/TiO_2 was 99.53, 94.51 and 89.27% during 1, 4, and 7 days of incubation, respectively. The efficiency of Ca-P-Ag/TiO_2 was compared to the samples synthesised without anodization and pre-treatment in $AgNO_3$ (one step Ca-P-Ag/TiO_2). The efficiency of one-step Ca-P-Ag/TiO_2 was lower (95.26, 69.22, 61.78% at 1, 4, and 7 days of incubation) as compared to the same with two-steps. For one-step Ca-P-Ag/TiO_2, the Ag content was lower, and it only existed on the surface of the coating. The two-step (pre-treatment and MAO) process could lead to the formation of micro-voids and micro-holes for the immobilization of Ag at the surface and inside the coating material. Microporous surface features could also enhance the hydrophilicity of the coating material. The fine pores on the surface could act as a barrier to delay the contact of body fluids with the antimicrobial Ag. Consequently, Ag content inside the coating material could be gradually released as it contacts with body fluids for long-term efficiency. The antimicrobial activity of the coating without Ag content was only 48.63% after 1 day. The antimicrobial action of two-steps Ca-P-Ag/TiO_2 was mainly attributed to coulomb force adsorption of Ag, steady-state release mechanism of antimicrobial agents, degradation of protein and photocatalytic reactions.

In a similar study, manganese (Mn) doped Ca-P/TiO_2 (Mn- Ca-P/TiO_2) was fabricated through a one-step MAO technique to evaluate the antimicrobial efficiency against *Staphylococcus aureus* [107]. Mn is one of the significant elements needed for bone growth, bone metabolism, synthesis of essential enzymes, and cellular homeostasis [108]. The ionic radius of Mn and Ca is analogous and hence it could be easily substituted in hydroxyapatite [109]. Consequently, Mn doping could considerably enhance the osseointegration of the Ti metal implant surface. Calcium acetate, ethylenediaminetetraacetic acid Mn disodium salt (Na_2Mn-EDTA), and sodium dihydrogen phosphate were used as precursors for the coating (Ti-Mn-EDTA). Coatings were also prepared with ethylenediaminetetraacetic acid tetra sodium salt for comparison (Ti-EDTA). Osteogenic activity of the coatings was assessed in MC3T3-E1 pre-osteoblast cells. The *in-vitro* bone formation capability of the coating was evaluated in simulated body fluid (SBF) at 37 °C for 1 week. A mixture of anatase and rutile phases of TiO_2 was observed. The percentage of rutile phase in Ti-Mn-EDTA was higher as compared to Ti-EDTA. Micro-nodules and nanopores were observed on the surface of both Ti-Mn-EDTA and Ti-EDTA. The pores were distributed uniformly and non-uniformly on the Ti-Mn-EDTA and Ti-Mn-EDTA coatings, respectively. The thickness of Ti-Mn-EDTA coatings (2.5 – 4 μm) was lower than Ti-Mn-EDTA (5 μm). XRD and XPS results suggested that Mn existed in the form of trimanganese tetroxide (Mn_3O_4) on TiO_2 coatings. The outer layer of Ti-Mn-EDTA coating was made of crystalline Mn_3O_4 with amorphous Ca-P, and the inner layer was composed of TiO_2. The phase composition of Ca and P was matched well with the hydroxyapatite. The water contact angle (WCA) and topography of the coatings are displayed in Fig. S7. WCA of Ti-Mn-EDTA (122°) was comparatively higher than that of Ti-EDTA (34°), indicating the coatings were hydrophobic after the incorporation of Mn. Topography results revealed that the surface roughness of Ti-Mn-EDTA (~1.5 μm) was higher than Ti-EDTA (~0.8 μm). The surface roughness could promote the adhesion of body cells and the deposition of hydroxyapatite on the implants. These electrochemical results showed that the corrosion resistance of Ti-Mn-EDTA was higher as compared to the Ti-EDTA and Ti substrate. The physical shielding effect of the coatings was ascribed to the deposition of a Ca-P phase.

The antibacterial rate histogram, photographs of *Staphylococcus aureus* colonies (after 24 h of incubation at 37 °C), and CLSM images of coating specimens are shown in Fig. S8. The antibacterial rate of Ti-Mn-EDTA was ~69.7%, whereas that of Ti-EDTA was ~56.9%. The viabilities of adherent microbes on the coated substrates were examined by the CLSM after 24 h of incubation. A high intensity of red fluorescence was observed for the Ti-Mn-EDTA coated substrate, indicating the presence of dead bacterial colonies. Inductively coupled plasma atomic emission spectroscopy (ICP-AES) results showed that Mn ionic release after 24 h of immersion was much lower than 0.01 ppm. Consequently, the antimicrobial property of Ti-Mn-EDTA was ascribed to the ROSs generation rather than Mn ionic release. The osteogenic activity of the coatings was evaluated after 1, 3 and 7 days. The cellular proliferation and relative growth rate of the Ti-Mn-EDTA coated substrate were higher than the Ti-EDTA and bare Ti substrate, signifying the influence of the MAO process and the active ingredients. The bone-forming capability of the coatings was examined in SBF at 37 °C for 1 week. A thick layer of hydroxyapatite and calcium titanate ($CaTiO_3$) crystals were observed on both coatings after the immersion period, indicating that both Ti-Mn-EDTA and Ti-EDTA could stimulate bone formation. The number of hydroxyapatite crystals on Ti-Mn-EDTA was slightly higher than that of Ti-EDTA. The doping of Mn could endorse the glycosaminoglycans synthesis [110] and bone-related marker gene expression [111] in osteoblasts to assist bone formation.

In another study, an anti-biofilm, biocompatible and superhydrophobic coating on Ti dental implants was engineered by a one-step non-thermal technique [112]. A low-pressure glow discharge plasma method was employed to minimize the polymicrobial bio-film adhesion on the Ti surface without influencing the fibroblast growth and proliferation. Hexamethyldisiloxane (HMDSO) was used as the surface functionalizing agent to impart superhydrophobic features. The antimicrobial property of the superhydrophobic Ti discs was evaluated for the *in vitro* bio-film inhibition in human saliva. According to the local research and ethical committee, the saliva samples were received from the five volunteers with good oral health. The salivary pellicle composition of the coatings was examined by proteomic analysis. Superhydrophobic Ti discs were in contact with the fresh human saliva for 2 h at 35 °C. Liquid chromatography quadrupole time-of-flight (LC-Q-TOF) was used to analyse the extracted proteins after the contact time. The fungal adhesion on the coatings was also investigated using *Candida albicans* (ATCC 90028). Biocompatibility of the coatings was assessed in fibroblast (F3T3-cells) embryonic swiss mouse cells. The microbial adhesion in biofilm could be improved by extracellular polymers produced by the *Streptococcus* species [113]. Therefore, the anti-biofilm activity of the Ti discs was also studied in *Streptococcus mutans* (UA 159) with 1% sucrose supplementation for 4 h. Lastly, the biofilm polymicrobial composition on the coating was examined to estimate around 40 bacteria species associated with periodontitis (a chronic infectious inflammation in the teeth) by checkerboard DNA-DNA hybridisation [114].

The surface of bare Ti disc was smoother whereas micrometre sized non-uniform aggregates (like cauliflower shape) were observed for superhydrophobic Ti disc. WCA of the superhydrophobic coating was higher than 150°, suggesting an influence from HDMSO and Ar/O_2 plasma treatment. Surface roughness parameters (such as average roughness (R_a), root mean square average (R_q), average maximum height (R_z), and maximum height (R_t)) of the superhydrophobic Ti disc were higher than that of the bare Ti disc. CLSM results revealed the higher surface area and increased number of peaks for the superhydrophobic Ti disc (coating thickness of ~18 nm with ~2. 5 μm peak height).

The superior corrosion resistance of the coating was shown *via* open circuit potential (−0.10 V ± 0.05 for the superhydrophobic Ti disc and −0.32 V ± 0.01) and impedance. The corrosion potential of superhydrophobic and bare Ti disc was −0.09 V ± 0.03 and −0.52 V ± 0.03, respectively. A total of 26 adsorbed proteins from saliva on both Ti discs were distinguished by proteomic analysis. Among them, 7 proteins were shared by both Ti discs. The bare Ti disc displayed a total of 18 proteins

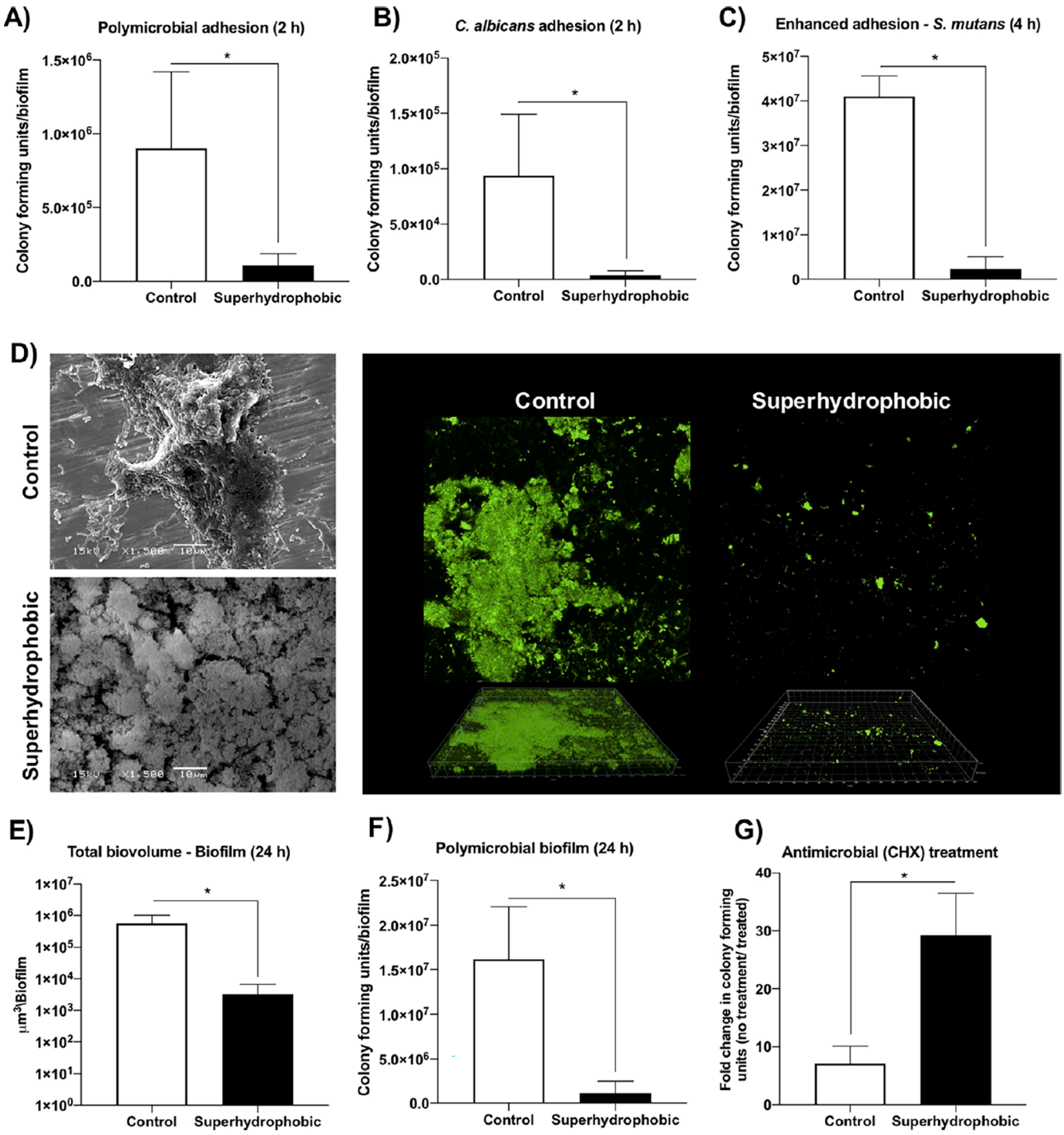

Fig. 9. *Invitro* antimicrobial activity of control and superhydrophobic Ti discs: (A) polymicrobial adhesion for 2 h, (B) fungal adhesion for 2 h, (C) *S. mutans* adhesion for 4 h, (D) SEM and the CLSM images of the biofilm, (E) average total biovolume of biofilms for 24 h, (F) average colony-forming units of polymicrobial biofilm for 24 h, and (G) average colony-forming units of biofilm for 24 h and exposed to chlorhexidine (0.5%) for 3 h [112]. Reproduced with permission from [112]. Copyrights (2020), American Chemical Society.

whereas the superhydrophobic Ti disc showed a total of 15 proteins, suggesting the differences in surface properties for protein adsorption. Fibroblast cell proliferation results at 1, 3 and 4 days suggested that the cell viability was not affected by both Ti discs, indicating the biocompatibility of the superhydrophobic Ti disc. *In-vitro* microbiological assay results (polymicrobial, fungal and *S. mutans* adhesion) and the CLSM images of biofilm on the Ti discs are shown in Fig. 9. CLSM images revealed that a dense polymicrobial biofilm adhesion was noted on the bare Ti disc, whereas very rare and thin microbial colonies were detected on the superhydrophobic Ti disc. Moreover, the biofilm formed on the superhydrophobic Ti disc was more susceptible to the antimicrobial agent chlorhexidine (0.5%) for 3 h. Total DNA levels of the 40 species on bare and superhydrophobic Ti discs were 130.4 ± 20.3 and 97 ± 68.7, respectively. Particularly, the level of *Campylobacter gracilis* pathogen (related to peri-implantitis and peri-implant bone loss in human) in the bare Ti disc was ~7-fold higher than the superhydrophobic Ti disc [115].

Recently, a 2D graphdiyne assembled TiO_2 nanofibers (TiO_2/GDY) was coated on Ti implants for bone tissue engineering [116]. GDY, owing to the presence of both *sp* and sp^2 hybridized carbon atoms, exhibits a large specific surface area with unique electrical conductivity and hole mobility. GDY was also reported for the visible-light-driven antimicrobial activity [117]. The antimicrobial (against MRSA biofilm formation) and osteogenic property of TiO_2/GDY were studied under *in-vitro* and *in-vivo* conditions. Plate counting results showed that ~98% MRSA colonies were disinfected by TiO_2/GDY under UV light irradiation (Fig. S9(a), and (b)). The microbial disinfection was not detected for the samples under dark conditions. The ratio of dead to living cells was four times higher for TiO_2/GDY compared to bare TiO_2 (Fig. S9(c), and (d)). SEM images revealed that biofilm formation was inhibited by the TiO_2/GDY + UV, and an intracellular ROSs generation was observed for the TiO_2/GDY treated bacteria (Fig. S9(e)). Fluorescence microscopy results revealed that the ROSs generation was increased with respect to irradiation time (Fig. S9(f) and (g)). The *in-vitro* osteogenic effect of TiO_2/GDY was studied using MC3T3-E1 cells. The results indicated that the nanocomposite exhibited more mineralization nodules and calcium deposition for a better osteoinduction. In addition, the cytotoxicity studies revealed an enhanced biocompatibility of the coatings. This was attributed to the presence of hydrophilic functional groups linked to the *sp* and sp^2 carbons which could strengthen the interaction of coatings with cells and proteins during tissue regeneration. The π conjugation and conjugated diacetylene bonds could develop a radical scavenging effect in GDY which makes them less cytotoxic in long-term use.

Fig. 10 shows the mechanism of photocatalytic antibacterial disinfection on TiO_2/GDY. During light irradiation, electrons and holes are formed on the surface of TiO_2 and GDY. The photo-generated electrons of TiO_2 could be easily transferred to the surface of GDY. There it can react with H_2O and O_2 to produce $^{\bullet}OH$ and $O_2^{\bullet-}$, indicating an enhanced ROSs generation through extending the lifetime of charge carriers. At the same time, the existence of GDY in the nanocomposite could promote bone tissue regeneration. Hence, the TiO_2/GDY composite could successfully be used for implant infections due to its sterilization effects and excellent biocompatibility. GDY was also reported for its free radical scavenging effect from long-term radiation-induced damage [118]. However, a significant amount of ROSs was generated by TiO_2/GDY for the disinfection of microbes. The authors suggested that a small amount of GDY was used in the nanocomposite (around 10 mg of GDY for 200 mg of TiO_2) and hence the impact of its free radical scavenging effect was negligible under a short irradiation time. Conversely, the free radical scavenging ability of TiO_2/GDY could be beneficial for long-term metal implantation with less cytotoxic effects compared to pure TiO_2.

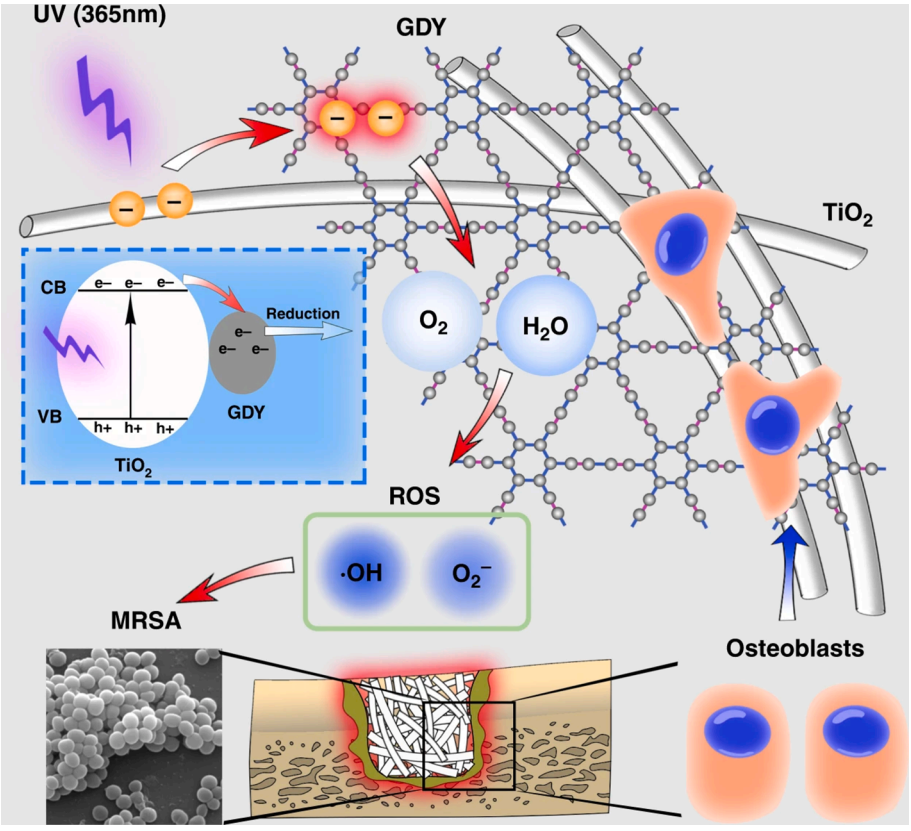

Fig. 10. TiO_2/GDY photocatalytic coatings for orthopaedic implant infection: Schematic of ROSs formation mechanism and biocompatibility [116]. Reproduced with permission from Ref. [116]. Copyrights (2020), Springer Nature.

4. Commercial antimicrobial coatings

4.1. Global challenges, problems and needs

Coating manufacturers have been covering their end-products with industrial coatings for many years, increasing the value of the end-product by conferring them numerous properties (anti-scratch, anti-corrosion, anti-fouling, durability, *etc*). But today manufacturers are facing a major challenge in the form of superbugs, viruses, and multi-drug resistant microbes. Superbugs are developing resistance to anti-microbials, outpacing the ability of the drug industry to develop new compounds. Thus, strategies are focusing on preventing the deposition and spread of these pathogens in society. Besides threatening health, these pathogens also damage production and infrastructure. Outlined below are some of the global challenges, problems and needs identified:

- Antimicrobial resistance refers to the ability of microbes (bacteria, viruses, fungi, parasites) to survive antimicrobial drugs and additives. Although this is a natural phenomenon, modern practices have accelerated it. Antimicrobial resistance is a major constraint and cost for healthcare systems worldwide.
- Some diseases can instigate pandemics, causing unprecedented economic, social, environmental, and sanitary impact.
- Mankind and animals share many infectious agents (zoonosis), which favours the expansion of resistant pathogens *via* the food chain, direct contact, or the environment. Global trade and travel increase the risk and are a public health concern.
- The main foodborne pathogens such as *Salmonella*, *Campylobacter* and *Escherichia coli* already showed resistance in pigs, cattle, and poultry. These superbugs are a threat to our health, the food industry, and our food supply.
- Antimicrobial alternatives to tackle the super-bugs are needed. The pharma industry is overwhelmed as it cannot keep pace with anti-microbial resistance. Microbes always manage to develop resistance.
- Prevention is the best option to address infectious diseases, since treatment is much more expensive.
- Infections need to be caught and fought early. Microbes create biofilms and colonize the surfaces of our infrastructure. These become dense colonies that display $\times$1000 times more resistance to antibiotics [119].
- The field needs innovative biocidal mechanisms. Most antibiotic drugs or additives target biological traits in the bacteria, which manage to overcome these agents which can result in mutation.
- The market requires antimicrobial coatings to protect surfaces from the spread of infections and the ability to mutate.

Contaminated surfaces contribute to the transmission of pathogens such as MRSA, *Escherichia coli, Clostridium difficile*, and clinically relevant viruses have been shown to survive on surfaces from hours to over a year [120]. The perpetrator of the most recent pandemic, SARS-CoV-2 has also been reported to survive for up to 28 days at 20 °C on common surfaces such as glass, stainless steel and both paper and polymer banknotes [121]. The impact caused by antimicrobial-resistant (AMR) pathogens is an international health epidemic. Globally it was estimated that 700,000 deaths could be attributed to AMR per annum and the annual toll will climb to 10 million in the next 30 years unless action is taken [122]. From an EU perspective, the death of 33,000 citizens is associated with AMR, resulting in €1.5 billion in healthcare and productivity losses, and equating to losses of US$ 100 trillion in global GDP by 2050 if nothing is done to reverse the trend [123]. However, the recent COVID-19 pandemic is a wakeup call, highlighting the wide-ranging socio-economic impact of such an outbreak [124].

4.2. Market landscape

According to market analysis, the global antimicrobial additives market size was valued at USD 2.6 billion in 2020 and is expected to grow at a compound annual growth rate (CAGR) of 8.4% to USD 4.3 billion in 2027 [please refer to reference S1 in supporting info]. Rapidly expanding end-use sectors due to a growing population and increased urbanisation are likely to escalate the demand for antimicrobial additives over the forecast period. Moreover, the continuously rising demand for healthcare and products to tackle the COVID-19 pandemic will positively impact market growth. The Asia Pacific is expected to dominate the market as the region has some of the major healthcare product manufacturers.

Despite government and public guidelines, measures such as social distancing, facemasks, and strict hygiene advice, it is extremely challenging to keep every surface continuously sanitized. Hence, there is a strong global requirement for self-sanitising properties that would neutralize the surface from contaminant pathogens and reduce the risk of possible spread. In 2020, the outbreak of COVID-19 has deeply impacted the global economy, however, the pandemic has a positive impact on the antimicrobial additives and products market. The development, application and use of anti-microbial coatings have quickly become hot topics, with more widespread adoption and increased interest driven particularly by the current COVID-19 crisis.

Antimicrobial coatings are being propelled by a blockage in the pharma industry, the emergence of multi-drug resistant pathogens and their rapid dissemination throughout the world *via* contact with consumer electronics, infrastructure, transport, food, or animals. Apart from the most important need to combat AMR, companies are seeking opportunities for USP, margin & sales growth, differentiation in crowded markets and innovation. Antimicrobial coatings with smart, environmental responsive, multifunctional features, such as continuous antimicrobial protection with scratch, abrasion, chemical and stain resistance with easy clean properties offers such opportunities.

The main market drivers include.

i) Emergence of antimicrobial resistance.
ii) Constraints in healthcare budgets.
iii) Focus on prevention.
iv) Globalisation of trade & travel.
v) An overwhelmed pharma industry that cannot find new antimicrobial drugs.
vi) Re-active response to finding solutions to the AMR crises through research, funding, healthcare, and industry.
vii) Opportunity for innovators to capitalise on a burgeoning demand with first-to-market products.
viii) Enhancement of corporate responsibility by delivery of social and environmentally compliant solutions.
ix) Access a global market opportunity backed by strong IP and robust stakeholder's strategy.
x) COVID-19 and societal demand.

Superbugs and viruses are becoming especially hazardous and costly for touch environments. The misuse of antimicrobials, either by not meeting the indications, diagnosis, administration or simply to cover for bad hygiene standards, has facilitated the selection and arrival of these pathogens which can display resistance to the battery of compounds available. Common infections may turn lethal if the agent becomes resistant to the indicated drug.

In the field of advanced coatings, several chemical manufacturers produce surface coatings. However, most of them do not possess an antimicrobial function. Although there is a list of companies that focus on antimicrobial coatings, they tend to include leaching agents in the formulation. There remain very few options to formulate coatings with antimicrobial properties. Most companies offer silver-based antimicrobial coatings. Available alternatives need UV light to activate the photocatalytic coating, which makes them only applicable to outdoor settings. The need for UV light influences the coating thickness since only longer wavelengths reach deeper sites of the layer. In turn,

thickness negatively influences the transparency and mechanical strength of the coating. Altogether, current coatings face drawbacks and limitations owing to the compounds used, fluidity, transparency, thickness, durability, and resistance in the presence of water/humidity.

The manufacturing sector has an urgent need for visible light activate non-silver containing antimicrobial coatings. This is driven by the highest regulatory standards in healthcare, food industry, construction, electronics, med-tech, pharma, public infrastructure, and home environments. There is a crucial need to prevent the spread of pathogen infections, which are a major concern due to the emergence of resistance and the threat of future pandemics.

4.3. Surface coating procedures

TiO_2 antimicrobial agents can be applied through standard dipping, spinning and spraying techniques or applied by chemical vapour deposition, sputtering, and thermal oxidation [38,125]. Each technique has advantages and drawbacks in terms of cost, manufacturability, and coating quality. TiO_2 can be applied in the amorphous phase and converted to other polymorphs on the substrate through heating, or it can be deposited in the already photocatalytic phase. The choice of TiO_2-based antimicrobial formulations will be dependent on the substrates of intended use *i.e.*, hard, or soft surfaces, and whether they are applied at a manufacturing stage, or as an aftermarket solution. The choice between binding agents, and physically sintering the TiO_2 crystals into a surface, such as glass or ceramic, could dramatically affect the durability of the coating.

4.4. Commercial antimicrobial coatings for medical implants

Commercially pure Ti and Ti-6Al-4V or grade 5 Ti are the most widely used biomedical metal implant. According to recent data, more than 1000 tonnes of Ti metal have been used for implants in patients every year [126]. Owing to the excellent biocompatibility, more than 50% of commercial Ti alloys are made up of Ti-6Al-4V (Titanium with 6 wt% aluminium and 4 wt% vanadium). In orthopaedics, Ti alloys have been used for hip/knee/elbow/shoulder joints, bone plates/screws/scaffolds, and spinal fusion cages. In addition to that, various Ti metal alloys (*e.g.*, Ti-6Al-7Nb, Ti-13Nb-13Zr, Ti-12Mo-6Zr-2Fe, Ti-15Mo, *etc*) have also been developed in recent years for biomedical applications. Bioactive agents such as gentamicin poly (d,l-lactide), silver, and povidone-iodine coatings were used to impart antimicrobial features in orthopaedic titanium implants (*e.g.* MUTARS®, implantcast, Germany) [127].

Ti dental implants in the commercial market have been manufactured by various techniques to tune their mechanical, antimicrobial and osseointegration characteristics. The surface microstructure and topography of Ti dental implants have been modified *via* sandblasting (e.g. TiOblast® (Astra Tech, Mölndal, Sweden)), anodization (e.g. TiUnite® (Nobel Biocare, Gothenburg, Sweden)), acid-etching (e.g. Steri-Oss Etched® (Nobel Biocare, Zürich-Flughafen, Switzerland)), plasma spraying (e.g. Steri-Oss-TPS® (Nobel Biocare, Yorba Linda, California, USA)), grit-blasting with acid etching (e.g. Friadent Plus® (Dentsply Friadent, Mannheim, Germany) and Osseospeed® (Dentsply Friadent, Mannheim, Germany)), and laser ablation (e.g. Laser-Lok® (Bio-Horizons, Birmingham, Alabama)) techniques to stimulate the osteointegration process. Materials such as calcium phosphate (e.g. Ossean® (Intra-Lock, Boca Raton, Florida, USA)), hydroxyapatite (e.g. TSV-HA® (Zimmer Biomet, Carlsbad, California, USA)), calcium nanoparticles, and calcium phosphate with discrete crystalline deposition (e.g. Nanotite® (Zimmer Biomet, Palm Beach Gardens, Florida, USA)) have been used as ceramic coatings on the Ti dental implants to promote the early bone healing [128].

4.5. Techno-economics and life cycle assessment

Techno-economy on the large-scale production of TiO_2 nanoparticles by the liquid-phase synthesis method has been recently analysed [129]. The feasibility was assessed through the engineering analysis (to assess the feasibility of large-scale production using the available technology and inexpensive apparatus) and economic evaluation (to estimate the profitability using the parameters like the payback period, profitability index, gross profit margin, cumulative net-present value, internal rate return, and break-even point). The project estimation was calculated with various parameters such as utilities, sales, raw materials, labour, taxes, and subsidiaries. The results showed the potential profitability of the project for the large-scale production of TiO_2. Nevertheless, further developments are required to attract investors and to increase the profit in developing countries. Moreover, the studies should also be focused on the synthesis of TiO_2 using bio-degradable raw materials to minimize waste and environmental burden.

Life cycle assessment (LCA) of TiO_2 coatings on residential window glass was examined using the Building of Environmental and Economic Sustainability (BEES) model [130]. The potential impact of TiO_2 on the environmental and economic aspects in a life cycle perspective (raw materials to final disposal) was evaluated [131]. Anatase TiO_2 was synthesised using a sol-gel technology, and the spray coating method was considered for the analysis. The indoor air quality, acidification potential, and smog formation potential of window glass were improved by the TiO_2 coating. The overall environmental score of TiO_2 coated glass was 0.44 (with an economic score of 0.52), whereas that of bare glass was 0.56 (with an economic score of 0.48), indicating the negative impact of TiO_2 coatings on the environment. In a similar study, the environmental impact of TiO_2 nanoparticles on recycled mortars was examined [132]. The life cycle assessment was focused on the production of materials to evaluate the sustainability of TiO_2 nanoparticles. The findings demonstrated that the addition of 0.5% of TiO_2 showed a significant reduction in global warming potential (GWP), suggesting the negative impact of TiO_2 on the environment. The incorporation of TiO_2 nanoparticles with recycled aggregates in concretes could also promote CO_2 uptake [132]. These studies suggest that the utilisation of TiO_2 coatings is beneficial during the whole life cycle.

5. Challenges and prospects

TiO_2 antimicrobial coatings are one of the promising remedies to disinfect or control the spread of potentially life-threatening pathogens from high-touch, shared surfaces as well as medical devices. Owing to the high surface to volume ratio of TiO_2 as well as the multitude of surface coating techniques, it could be easily applied as a surface coating to destroy the toxic pathogens for the long-term. The technical challenges in antimicrobial surface coatings may offer a plethora of opportunities for the innovation and development in medical devices [133], sensors [134–136], membranes [137], food packaging [138], *etc*.

Stability/durability: The lifespan of TiO_2 antimicrobial coatings entirely relies on the type of application. For instance, the antimicrobial features of high touch surfaces should be considered for at least a year. In the case of surgical or medical devices, the antimicrobial property should be confined to a few hours, whereas for the medical implant the efficacy of TiO_2 must be limited to the necessary period of the body to accept the implant. The stability and durability of the photocatalytic coatings should be regularly monitored to guarantee their efficacy against the pathogens.

Coating methods: Spraying techniques have been primarily utilised to coat TiO_2 on various surfaces. Nevertheless, inkjet printing, and hydrothermal synthesis and liquid phase deposition would be some of the most convenient methods in the future to coat or print TiO_2 materials, as TiO_2 could then be incorporated into bioprinting or onto 3-D printed components, which is gaining popularity as additively manufactured implantable become more commonplace [139]. Most of the

photocatalytic coatings are biocompatible at a particular concentration with a specific coating method, however in-depth cytotoxic analysis should be required to evaluate the safety features of antimicrobial nanomaterials.

Analytical tools: Sophisticated instruments are available in the contemporary world for the rapid identification of pathogens in any kind of environment. However, the recent COVID-19 pandemic has proven that additional pioneering materials or technologies should be instigated soon to safeguard the human race from any kind of infectious virus (*e.g.*, enveloped, non-enveloped, RNA based, etc) and multi-drug resistant strains.

Antibiotic-resistant strains: Alexander Fleming warned about the emergence of antibiotic-resistant strains during the discovery of penicillin. After the 2000s it was evident that the evolution of antibiotic-resistant strains from the extensive dissemination of various antibiotics. For instance, Ag resistant genes were identified in the clinical isolates of *Enterobacter* and *Klebsiella* species in Swedish healthcare facilities [140]. Experts have already warned about the link between COVID-19 and antibiotic-resistant microbes [141,142]. Few countries have reported an increased number of cases related to multi-drug resistant microbes during the COVID-19 pandemic [141,143–146]. The execution of light-active TiO_2 coatings is an outstanding option to fight against the antibiotic-resistant strains developed in several environments such as shared touch surfaces, healthcare environments, water resources, agriculture, food, *etc*. Future studies should focus on dealing with these various antibiotic-resistant pathogens with innovative antimicrobial surfaces.

Regulations: One of the major challenges is the shortage of standard protocols to evaluate the antimicrobial features and long-term efficiency of innovative materials, suggesting the difficulty in comparing the activity of novel materials with existing products in the market/R&D. In the current scenario, the photocatalytic products must be approved by the major regulatory bodies such as the Environmental Protection Agency (EPA) and The United States Food and Drug Administration (FDA). The product regulations (e.g., biocidal products regulation EU 528/2012, EC No. 1907/2006, *etc*) for the antimicrobial coatings or biocidal materials are time consuming and expensive, and therefore it is vital to instigate the standard protocols for the speedy transition of novel antimicrobial strategies from the lab to industries and commercial market.

Commercialization [23]: Kastus®, GermstopSQ, Green Millennium, NanoSeptic, Berger Elegance, GERM ARMOR®, TiTANO®, Titano-Clean®, DrivePur, PureTi, PALCCOAT, TOTO, Pilkington SaniTise™, and airlite are the approved photocatalytic products or coatings in the market for antimicrobial applications. Further developments on photocatalysis or similar eco-friendly techniques could reduce the risk of another 'apocalyptic threat' by the spread of pathogens.

A recent study suggested that most of the commercially available Ti implants with antimicrobial features have been limited only to orthopaedics. The mechanical durability and antimicrobial property of dental implants may vary as compared to that of orthopaedic implants. Therefore, extensive research efforts should be taken in dental implantology to improve the long-term antimicrobial features of titanium dental implants.

Surface features: Superhydrophilic TiO_2 coatings could effectively disinfect pathogens under light illumination. Nonetheless, a thick layer of biofilm might be developed under dark conditions (for example at night time), which could cease the photocatalytic efficacy of the coatings by blocking the photocatalytic reaction at the surface [147]. Henceforth, the surface coatings with the combination of superhydrophobic and antiviral features would be the ideal option in the future to furnish a double layer of protection against infectious microbes. The superhydrophobic characteristics could avoid the adhesion of the majority of microbes, and the antiviral ingredients could inactivate the remaining microbes adhered on the surface. These coatings could also be used in the food and medical industries to significantly reduce the number of pathogens spreading from person to person.

Mechanism: The entry of ROSs or active metals into the cell may differ with respect to the structural features of the microbes, and there are very limited studies on endocytosis. All the vulnerable biocomponents to microbes during the ROSs attack should be investigated in detail to attain the maximum antimicrobial efficacy without regrowth. Only a few studies are focused on the intracellular mechanisms and the attack of ROSs on microbial genes. The photocatalytic disinfection efficacy of parental microbial strains and their genomic mutants should be compared to enrich the activity of coatings. Besides the antioxidative enzymes, the capsular epoxy polysaccharides (EPS) could also safeguard the microbes from the ROSs attack [148]. Extensive studies are required for the in-depth knowledge of microbial disinfection mechanism using cytobiology and genetic technology.

Cytotoxicity: The mechanism for the genotoxicity and cytotoxicity of non-bound TiO_2 particles should be comprehensively studied on various cell lines to investigate any potential toxic effects. Cytotoxicity could be influenced by the shape, size, and crystal structure of TiO_2. Reliable toxicokinetic models should be developed to assess the viability of antimicrobial photocatalytic coatings. To validate the safety features of the antimicrobial coatings, the toxic effects of TiO_2 nanoparticles interacting with other compounds should be studied. Compared to chemical approaches, green chemistry would be favourable for the synthesis of metal oxide nanoparticles with low cytotoxicity for long-term antimicrobial applications.

Some of the Ti metal implants might cause allergic symptoms such as irritation, erythema, and inflammation, leading to reactions such as yellow nail syndrome [149]. The release of metal ions into human blood after several months of implant placement has been observed and the binding of these metal ions to biomolecules might cause a severe toxic effect. The toxicity, bioavailability, and environmental impact of Ti/TiO_2 have been recently reviewed [150]. The report suggested that TiO_2 rarely cause health and environmental problems. However, the influence of TiO_2 on biodiversity, terrestrial and aquatic ecosystems should be investigated in detail in the future.

Innovations: There are no comprehensive reports on the antimicrobial efficacy of surgical or laboratory gloves, indicating the negative impact of nanoparticles on the physio-chemical properties of latex. Antimicrobial gloves would be considered as one significant area to explore in the future. In the coming decades, a lot of innovations could ensue on the antimicrobial features of 2D materials such as graphene, MXenes, layered double hydroxides, and graphitic-carbon nitride.

6. Summary

TiO_2 photocatalysis can be considered as the most sustainable, biocompatible, and cost-effective technologies to deactivate infectious pathogens with superior efficiency on various surfaces. Herein, the recent advances of the antimicrobial TiO_2 nanocomposite coatings for surfaces, and medical implants have been reviewed.

Cell membrane rupture, leakage of K^+ ions, the decline of antioxidative enzymes/ATP concentration, and the damage of genome DNA/cytoplasm are the significant steps for the bacteria-killing mechanism. The photocatalytic disinfection of viruses is usually explored *via* analysing the damage of major building blocks such as RNA and surface proteins. The antimicrobial efficiency of the coatings could be mainly influenced by humidity, temperature, light illumination, and the accessibility of O_2.

In most cases, TiO_2 is doped with metals (*e.g.*, P, F, Cu, Ag, *etc*) or hybridised with 2D materials (e.g., MXenes, MOFs) to enrich the electron-hole separation process to achieve the maximum disinfection. The antimicrobial activity is mainly influenced by the discrepancy of microbe and coating material surface characteristics (*e.g.*, electrostatic interaction, pH, topology, *etc*). The reactivation or regrowth of microbes was not spotted on the TiO_2 coatings after the light illumination. The crystalline features of TiO_2 such as facets and oxygen vacancies could be

able to impact the yield of ROSs generation during photocatalysis.

TiO_2 antimicrobial coatings could be utilised in dental and orthopaedic implants owing to its outstanding characteristics. TiO_2 antimicrobial coatings on the metal implants are biocompatible without any cytotoxicity. The surface roughness of the coating could promote the adhesion of body cells and stimulate bone formation through the deposition of hydroxyapatite on the implants. Components such as Ca, P, Mn, Ag and 2D materials were used to enrich the antimicrobial applications of TiO_2 coatings. MAO is an economically viable method to control the composition of coating elements and introduce porous features on the Ti implants to enhance the growth of osteoblasts. Silane functionalizing agents and polymers are commonly used to create superhydrophobicity in metal implants to avoid the adhesion of microbes.

The COVID-19 pandemic situation has created an extra burden on the global health systems to determine the antimicrobial strategies to curtail the spread of coronavirus and other emerging pathogens. TiO_2 surface coating is an impressive technology to deal with health issues caused by life-threatening pathogen infections. TiO_2 surface coatings might be used to prevent the spread of pathogens in high-risk public areas with shared contact surfaces such as train stations, bus stations, airport, schools, colleges, stadiums, hospitals, religious places, supermarkets, theatres, museums, malls, libraries, hotels, bars, swimming pools, *etc*.

Declaration of Competing Interest

The authors declare that they have no known competing financial interests or personal relationships that could have appeared to influence the work reported in this paper.

Acknowledgments

The authors (VK, SM, JB and SCP) would like to thank the European Union's INTERREG VA Programme for the Renewable Engine (RE) project, managed by the Special EU Programmes Body (SEUPB), with match funding provided by the Department for the Economy (Northern Ireland) and Department of Enterprise, Trade and Employment (Republic of Ireland). The authors (JEK, HGM, BW, and NL) would like to thank H2020 EIC Accelerator fund under the project name SPYGLASS (Project number 959211) and Science Foundation Ireland (SFI) under Grant 18/IF/6324.

Appendix A. Supplementary data

Supplementary data to this article can be found online at https://doi.org/10.1016/j.cej.2021.129071.

References

[1] E. Horváth, L. Rossi, C. Mercier, C. Lehmann, A. Sienkiewicz, L. Forró, Photocatalytic nanowires-based air filter: towards reusable protective masks, Adv. Funct. Mater. 30 (2020) 2004615.
[2] S. Lu, G. Meng, C. Wang, H. Chen, Photocatalytic inactivation of airborne bacteria in a polyurethane foam reactor loaded with a hybrid of MXene and anatase TiO_2 exposing {001} facets, Chem. Eng. J. 404 (2020), 126526.
[3] K.G. Andersen, A. Rambaut, W.I. Lipkin, E.C. Holmes, R.F. Garry, The proximal origin of SARS-CoV-2, Nat. Med. 26 (2020) 450–452.
[4] X. Lu, L. Zhang, H. Du, J. Zhang, Y.Y. Li, J. Qu, W. Zhang, Y. Wang, S. Bao, Y. Li, SARS-CoV-2 infection in children, N. Engl. J. Med. 382 (2020) 1663–1665.
[5] D. Pinto, Y.-J. Park, M. Beltramello, A.C. Walls, M.A. Tortorici, S. Bianchi, S. Jaconi, K. Culap, F. Zatta, A. De Marco, Cross-neutralization of SARS-CoV-2 by a human monoclonal SARS-CoV antibody, Nature 583 (2020) 290–295.
[6] T.T. Le, Z. Andreadakis, A. Kumar, R.G. Roman, S. Tollefsen, M. Saville, S. Mayhew, The COVID-19 vaccine development landscape, Nat. Rev. Drug Discov. 19 (2020) 305–306.
[7] N. Lurie, M. Saville, R. Hatchett, J. Halton, Developing Covid-19 vaccines at pandemic speed, N. Engl. J. Med. 382 (2020) 1969–1973.
[8] M.D. Shin, S. Shukla, Y.H. Chung, V. Beiss, S.K. Chan, O.A. Ortega-Rivera, D. M. Wirth, A. Chen, M. Sack, J.K. Pokorski, COVID-19 vaccine development and a potential nanomaterial path forward, Nat. Nanotechnol. 15 (2020) 646–655.
[9] C.A. Bode-Aluko, O. Pereao, H.H. Kyaw, L. Al-Naamani, M.Z. Al-Abri, M.T. Z. Myint, A. Rossouw, O. Fatoba, L. Petrik, S. Dobretsov, Photocatalytic and antifouling properties of electrospun TiO_2 polyacrylonitrile composite nanofibers under visible light, Mater. Sci. Eng., B 264 (2021), 114913.
[10] K. Wojciechowski, M. Gutarowicz, J. Mierzejewska, P. Parzuchowski, Antimicrobial films of poly (2-aminoethyl methacrylate) and its copolymers doped with TiO_2 and $CaCO_3$, Colloids Surf. B185 (2020), 110605.
[11] S. Khaiboullina, T. Uppal, N. Dhabarde, V.R. Subramanian, S.C. Verma, Inactivation of human coronavirus by Titania nanoparticle coatings and UVC radiation: throwing light on SARS-CoV-2, Viruses 13 (2021) 19.
[12] N. Yoshizawa, R. Ishihara, D. Omiya, M. Ishitsuka, S. Hirano, T. Suzuki, Application of a photocatalyst as an inactivator of bovine coronavirus, Viruses 12 (2020) 1372.
[13] O. Negrete, S. Bradfute, S.R. Larson, A. Sinha, K.R. Coombes, R.S. Goeke, L.A. Keenan, J. Duay, M. Van Heukelom, S. Meserole, Photocatalytic Material Surfaces for SARS-CoV-2 Virus Inactivation. No. SAND2020-9861. Sandia National Lab. (SNL-CA), Livermore, CA (United States); Sandia National Lab.(SNL-NM), Albuquerque, NM (United States), 2020.
[14] S. Zhang, X. Liang, G.M. Gadd, Q.i. Zhao, Advanced titanium dioxide-polytetrafluorethylene (TiO_2-PTFE) nanocomposite coatings on stainless steel surfaces with antibacterial and anti-corrosion properties, Appl. Surf. Sci. 490 (2019) 231–241.
[15] Q.i. Zhao, C. Liu, X. Su, S. Zhang, W. Song, S.u. Wang, G. Ning, J. Ye, Y. Lin, W. Gong, Antibacterial characteristics of electroless plating Ni–P–TiO_2 coatings, Appl. Surf. Sci. 274 (2013) 101–104.
[16] C. Liu, L. Geng, Y. Yu, Y. Zhang, B. Zhao, Q. Zhao, Mechanisms of the enhanced antibacterial effect of Ag-TiO_2 coatings, Biofouling 34 (2018) 190-199.
[17] C. Liu, L. Geng, Y. Yu, Y. Zhang, B. Zhao, S. Zhang, Q.i. Zhao, Reduction of bacterial adhesion on Ag-TiO_2 coatings, Mater. Lett. 218 (2018) 334–336.
[18] S. Veltri, A.M. Palermo, G. De Filpo, F. Xu, Subsurface treatment of TiO_2 nanoparticles for limestone: prolonged surface photocatalytic biocidal activities, Build. Environ. 149 (2019) 655–661.
[19] B.E. Nagay, C. Dini, J.M. Cordeiro, A.n.P. Ricomini-Filho, E.D. De Avila, E.C. Rangel, N.C. Da Cruz, V.A. Barão, Visible-light-induced photocatalytic and antibacterial activity of TiO_2 codoped with nitrogen and bismuth: new perspectives to control implant-biofilm-related diseases, ACS Appl. Mater. Interfaces, 11 (2019) 18186-18202.
[20] K. Zheng, S. Li, L. Jing, P.Y. Chen, J. Xie, Synergistic Antimicrobial Titanium Carbide (MXene) conjugated with gold nanoclusters, Adv. Healthcare Mater. 9 (2020) 2001007.
[21] J. Yang, C. Wang, X. Liu, Y. Yin, Y.H. Ma, Y. Gao, Y. Wang, Z. Lu, Y. Song, Gallium-carbenicillin framework coated defect-rich hollow TiO_2 as a photocatalyzed oxidative stress amplifier against complex infections, Adv. Funct. Mater. 30 (2020) 2004861.
[22] E.A. Dil, M. Ghaedi, A. Asfaram, F. Mehrabi, A.A. Bazrafshan, L. Tayebi, Synthesis and application of Ce-doped TiO_2 nanoparticles loaded on activated carbon for ultrasound-assisted adsorption of Basic Red 46 dye, Ultrason. Sonochem. 58 (2019), 104702.
[23] S.M. Imani, L. Ladouceur, T. Marshall, R. Maclachlan, L. Soleymani, T.F. Didar, Antimicrobial nanomaterials and coatings: current mechanisms and future perspectives to control the spread of viruses including SARS-CoV-2, ACS Nano 14 (2020) 12341–12369.
[24] R. Chen, M.D. Willcox, K.K.K. Ho, D. Smyth, N. Kumar, Antimicrobial peptide melimine coating for titanium and its in vivo antibacterial activity in rodent subcutaneous infection models, Biomaterials 85 (2016) 142–151.
[25] H. Qu, C. Knabe, S. Radin, J. Garino, P. Ducheyne, Percutaneous external fixator pins with bactericidal micron-thin sol–gel films for the prevention of pin tract infection, Biomaterials 62 (2015) 95–105.
[26] D. McShan, P.C. Ray, H. Yu, Molecular toxicity mechanism of nanosilver, J. Food Drug Anal. 22 (2014) 116–127.
[27] H.H. Tuson, D.B. Weibel, Bacteria–surface interactions, Soft Matter 9 (2013) 4368–4380.
[28] D. Banerjee, P. Shivapriya, P.K. Gautam, K. Misra, A.K. Sahoo, S.K. Samanta, A review on basic biology of bacterial biofilm infections and their treatments by nanotechnology-based approaches, Proc. Natl. Acad. Sci., India, Sect. B Biol. Sci. 90 (2019) 243–259.
[29] S.T. Rutherford, B.L. Bassler, Bacterial quorum sensing: its role in virulence and possibilities for its control, Cold Spring Harb Perspect Med 2 (2012) a012427.
[30] K. Li, J. Qian, P. Wang, C. Wang, B. Lu, W. Jin, X. He, S. Tang, C. Zhang, P. Gao, Responses of freshwater biofilm formation processes (from colonization to maturity) to anatase and rutile TiO_2 nanoparticles: effects of nanoparticles aging and transformation, Water Res. 182 (2020), 115953.
[31] P. Makvandi, C.Y. Wang, E.N. Zare, A. Borzacchiello, L.N. Niu, F.R. Tay, Metal-based nanomaterials in biomedical applications: antimicrobial activity and cytotoxicity aspects, Adv. Funct. Mater. 30 (2020) 1910021.
[32] B. Di Credico, I. Bellobono, M. D'Arienzo, D. Fumagalli, M. Redaelli, R. Scotti, F. Morazzoni, Efficacy of the reactive oxygen species generated by immobilized TiO_2 in the photocatalytic degradation of diclofenac, Int. J. Photoenergy 2015 (2015), 919217.
[33] V. Etacheri, C. Di Valentin, J. Schneider, D. Bahnemann, S.C. Pillai, Visible-light activation of TiO_2 photocatalysts: advances in theory and experiments, J. Photochem. Photobiol., C 25 (2015) 1–29.
[34] J. Zhang, Y. Nosaka, Mechanism of the OH radical generation in photocatalysis with TiO2 of different crystalline types, J. Phys. Chem. C 118 (2014) 10824-10832.

[35] S.C. Pillai, P. Periyat, R. George, D.E. McCormack, M.K. Seery, H. Hayden, J. Colreavy, D. Corr, S.J. Hinder, Synthesis of high-temperature stable anatase TiO_2 photocatalyst, J. Phys. Chem. C 111 (2007) 1605-1611.

[36] D.A.H. Hanaor, C.C. Sorrell, Review of the anatase to rutile phase transformation, J Mater Sci 46 (2011) 855-874.

[37] F. Cao, J. Xiong, F. Wu, Q. Liu, Z. Shi, Y. Yu, X. Wang, L. Li, Enhanced photoelectrochemical performance from rationally designed anatase/rutile TiO_2 heterostructures, ACS Appl. Mater. Interfaces 8 (2016) 12239-12245.

[38] N.S. Leyland, J. Podporska-Carroll, J. Browne, S.J. Hinder, B. Quilty, S.C. Pillai, Highly efficient F, Cu doped TiO_2 anti-bacterial visible light active photocatalytic coatings to combat hospital-acquired infections, Sci. Rep. 6 (2016) 24770.

[39] Y. Nosaka, A.Y. Nosaka, Generation and detection of reactive oxygen species in photocatalysis, Chem. Rev. 117 (2017) 11302–11336.

[40] Y. Yan, C. Soraru, V.R. Keller, N. Keller, L. Ploux, Antibacterial and biofilm-preventive photocatalytic activity and mechanisms on P/F-modified TiO_2 coatings, ACS Appl. Bio Mater. 3 (2020) 5687-5698.

[41] F. Achouri, M.B. Said, M.A. Wahab, L. Bousselmi, S. Corbel, R. Schneider, A. Ghrabi, Effect of photocatalysis (TiO_2/UVA) on the inactivation and inhibition of Pseudomonas aeruginosa virulence factors expression, Environ. Technol. 1–10 (2020).

[42] K.A. Saharudin, S. Sreekantan, N. Basiron, Y.L. Khor, N.H. Harun, R.B.S.M. N. Mydin, H. Md Akil, A. Seeni, K. Vignesh, Bacteriostatic activity of LLDPE nanocomposite embedded with sol-gel synthesized TiO_2/ZnO coupled oxides at various ratios, Polymers 10 (2018) 878.

[43] E.O. Ogunsona, R. Muthuraj, E. Ojogbo, O. Valerio, T.H. Mekonnen, Engineered nanomaterials for antimicrobial applications: a review, Appl. Mater. Today 18 (2020) 100473.

[44] M.S.I. Khan, S.-W. Oh, Y.-J. Kim, Power of scanning electron microscopy and energy dispersive X-ray analysis in rapid microbial detection and identification at the single cell level, Sci. Rep. 10 (2020) 2368.

[45] L. Jiang, Y. Wen, Z. Zhu, C. Su, S. Ye, J. Wang, X. Liu, W. Shao, Construction of an efficient nonleaching graphene nanocomposites with enhanced contact antibacterial performance, Chem. Eng. J. 382 (2020), 122906.

[46] C. Zhang, Y. Li, D. Shuai, Y. Shen, W. Xiong, L. Wang, Graphitic carbon nitride (g-C_3N_4)-based photocatalysts for water disinfection and microbial control: a review, Chemosphere 214 (2019) 462–479.

[47] H. Zhao, H. Yu, X. Quan, S. Chen, Y. Zhang, H. Zhao, H. Wang, Fabrication of atomic single layer graphitic-C_3N_4 and its high performance of photocatalytic disinfection under visible light irradiation, Appl. Catal., B 152 (2014) 46–50.

[48] G. Li, X. Nie, J. Chen, Q. Jiang, T. An, P.K. Wong, H. Zhang, H. Zhao, H. Yamashita, Enhanced visible-light-driven photocatalytic inactivation of Escherichia coli using g-C_3N_4/TiO_2 hybrid photocatalyst synthesized using a hydrothermal-calcination approach, Water Res. 86 (2015) 17–24.

[49] J. Deng, J. Liang, M. Li, M. Tong, Enhanced visible-light-driven photocatalytic bacteria disinfection by g-C_3N_4-AgBr, Colloids Surf. B 152 (2017) 49–57.

[50] J.A. Byrne, P.A. Fernandez-Ibanez, P.S. Dunlop, D. Alrousan, J.W. Hamilton, Photocatalytic enhancement for solar disinfection of water: a review, Int. J. Photoenergy 2011 (2011), 798051.

[51] K.L. Nelson, A.B. Boehm, R.J. Davies-Colley, M.C. Dodd, T. Kohn, K.G. Linden, Y. Liu, P.A. Maraccini, K. McNeill, W.A. Mitch, Sunlight-mediated inactivation of health-relevant microorganisms in water: a review of mechanisms and modeling approaches, Environ. Sci. Processes Impacts 20 (2018) 1089–1122.

[52] D. Xia, Z. Shen, G. Huang, W. Wang, J.C. Yu, P.K. Wong, Red phosphorus: an earth-abundant elemental photocatalyst for "green" bacterial inactivation under visible light, Environ. Sci. Technol. 49 (2015) 6264–6273.

[53] Y. Li, C. Zhang, D. Shuai, S. Naraginti, D. Wang, W. Zhang, Visible-light-driven photocatalytic inactivation of MS2 by metal-free g-C_3N_4: virucidal performance and mechanism, Water Res. 106 (2016) 249–258.

[54] M. Lettieri, D. Colangiuli, M. Masieri, A. Calia, Field performances of nanosized TiO_2 coated limestone for a self-cleaning building surface in an urban environment, Build. Environ. 147 (2019) 506–516, https://doi.org/10.1016/j.buildenv.2018.10.037.

[55] N. Liu, Q. Zhu, N. Zhang, C. Zhang, N. Kawazoe, G. Chen, N. Negishi, Y. Yang, Superior disinfection effect of Escherichia coli by hydrothermal synthesized TiO_2-based composite photocatalyst under LED irradiation: influence of environmental factors and disinfection mechanism, Environ. Pollut. 247 (2019) 847–856.

[56] Y. Wang, L. Rao, P. Wang, Z. Shi, L. Zhang, Photocatalytic activity of N-TiO_2/O-doped N vacancy g-C_3N_4 and the intermediates toxicity evaluation under tetracycline hydrochloride and Cr (VI) coexistence environment, Appl. Catal., B 262 (2020), 118308.

[57] J. Zhang, L. Jiang, D. Wu, Y. Yin, H. Guo, Effects of environmental factors on the growth and microcystin production of Microcystis aeruginosa under TiO_2 nanoparticles stress, Sci. Total Environ. 734 (2020) 139443.

[58] T. Zeller, Detoxification of hydrogen peroxide and expression of catalase genes in Rhodobacter, Microbiology 150 (2004) 3451–3462.

[59] M.R. Groves, D. Lucana, Adaptation to oxidative stress by Gram-positive bacteria: the redox sensing system HbpS-SenS-SenR from Streptomyces reticuli, Appl. Microbiol. Microb. Biotechnol. 1 (2010) 33–42.

[60] A. Alhasawi, Z. Castonguay, N.D. Appanna, C. Auger, V.D. Appanna, Glycine metabolism and anti-oxidative defence mechanisms in Pseudomonas fluorescens, Microbiol. Res. 171 (2015) 26–31, https://doi.org/10.1016/j.micres.2014.12.001.

[61] J. Qiu, S. Li, E. Gray, H. Liu, Q.-F. Gu, C. Sun, C. Lai, H. Zhao, S. Zhang, Hydrogenation synthesis of blue TiO_2 for high-performance lithium-ion batteries, J. Phys. Chem. C 118 (2014) 8824-8830.

[62] C. Di Valentin, G. Pacchioni, A. Selloni, Reduced and n-type doped TiO2: nature of Ti3+ species, J. Phys. Chem. C 113 (2009) 20543-20552.

[63] H. Guo, S. Tan, J. Gao, L. Wang, Sequential release of drugs form a dual-delivery system based on pH-responsive nanofibrous mats towards wound care, J. Mater. Chem. B 8 (2020) 1759–1770.

[64] C.H. Goss, Y. Kaneko, L. Khuu, G.D. Anderson, S. Ravishankar, M.L. Aitken, N. Lechtzin, G. Zhou, D.M. Czyz, K. McLean, O. Olakanmi, H.A. Shuman, M. Teresi, E. Wilhelm, E. Caldwell, S.J. Salipante, D.B. Hornick, R.J. Siehnel, L. Becker, B.E. Britigan, P.K. Singh, Gallium disrupts bacterial iron metabolism and has therapeutic effects in mice and humans with lung infections, Sci. Transl. Med. 10 (2018) eaat7520.

[65] S.-r. Choi, B.E. Britigan, P. Narayanasamy, Dual Inhibition of Klebsiella pneumoniae and Pseudomonas aeruginosa Iron Metabolism Using Gallium Porphyrin and Gallium Nitrate, ACS Infect. Dis. 5 (2019) 1559-1569.

[66] J. Singh, S. Jadhav, S. Avasthi, P. Sen, Designing photocatalytic nanostructured antibacterial surfaces: why is black silica better than black silicon? ACS Appl. Mater. Interfaces 12 (2020) 20202–20213.

[67] E.P. Ivanova, J. Hasan, H.K. Webb, G. Gervinskas, S. Juodkazis, V.K. Truong, A.H. F. Wu, R.N. Lamb, V.A. Baulin, G.S. Watson, J.A. Watson, D.E. Mainwaring, R. J. Crawford, Bactericidal activity of black silicon, Nat. Commun. 4 (2013) 2838.

[68] Q. Tan, F. Lu, C. Xue, W. Zhang, L. Lin, J. Xiong, Nano-fabrication methods and novel applications of black silicon, Sens. Actuators, A 295 (2019) 560–573.

[69] S.K. Saini, M. Halder, Y. Singh, R.V. Nair, Bactericidal characteristics of bioinspired nontoxic and chemically stable disordered silicon nanopyramids, ACS Biomater. Sci. Eng. 6 (2020) 2778–2786.

[70] D.P. Linklater, M. De Volder, V.A. Baulin, M. Werner, S. Jessl, M. Golozar, L. Maggini, S. Rubanov, E. Hanssen, S. Juodkazis, E.P. Ivanova, High Aspect Ratio Nanostructures Kill Bacteria via Storage and Release of Mechanical Energy, ACS Nano 12 (2018) 6657-6667.

[71] J.J. Dong, A. Muszanska, F. Xiang, R. Falkenberg, B. van de Belt-Gritter, T. Loontjens, Contact killing of gram-positive and gram-negative bacteria on PDMS provided with immobilized hyperbranched antibacterial coatings, Langmuir 35 (2019) 14108–14116.

[72] M. Rosales, T. Zoltan, C. Yadarola, E. Mosquera, F. Gracia, A. García, The influence of the morphology of 1D TiO_2 nanostructures on photogeneration of reactive oxygen species and enhanced photocatalytic activity, J. Mol. Liq. 281 (2019) 59–69.

[73] D. Cheng, Y. Li, L. Yang, S. Luo, L. Yang, X. Luo, Y. Luo, T. Li, J. Gao, D. D. Dionysiou, One–step reductive synthesis of Ti3+ self–doped elongated anatase TiO_2 nanowires combined with reduced graphene oxide for adsorbing and degrading waste engine oil, J. Hazard. Mater. 378 (2019), 120752.

[74] C. Li, L. Ren, X. Liu, C. Zhang, D. Chen, W. Xu, Y. Qin, Superhydrophilic and underwater superoleophobic poly(propylene) nonwoven coated with TiO_2 by atomic layer deposition, Adv. Mater. Interfaces 8 (2020) 2001485.

[75] Z. Gong, N. Yang, Z. Chen, B. Jiang, Y. Sun, X. Yang, L. Zhang, Fabrication of meshes with inverse wettability based on the TiO_2 nanowires for continuous oil/water separation, Chem. Eng. J. 380 (2020), 122524.

[76] T.-D. Pham, B.-K. Lee, Effects of Ag doping on the photocatalytic disinfection of E. coli in bioaerosol by Ag–TiO_2/GF under visible light, J. Colloid Interface Sci. 428 (2014) 24–31.

[77] L. Gu, J. Wang, H. Cheng, Y. Zhao, L. Liu, X. Han, One-step preparation of graphene-supported anatase TiO_2 with exposed {001} facets and mechanism of enhanced photocatalytic properties, ACS Appl. Mater. Interfaces 5 (2013) 3085-3093.

[78] Q. Luo, B. Chai, M. Xu, Q. Cai, Preparation and photocatalytic activity of TiO_2-loaded Ti_3C_2 with small interlayer spacing, Appl. Phys. A 124 (2018) 495.

[79] Y. Sun, X. Meng, Y. Dall'Agnese, C. Dall'Agnese, S. Duan, Y. Gao, G. Chen, X.-F. Wang, 2D MXenes as Co-catalysts in photocatalysis: synthetic methods, Nano-Micro Lett. 11 (2019) 79.

[80] M. Sansotera, S. Geran Malek Kheyli, A. Baggioli, C.L. Bianchi, M.P. Pedeferri, M. V. Diamanti, W. Navarrini, Absorption and photocatalytic degradation of VOCs by perfluorinated ionomeric coating with TiO_2 nanopowders for air purification, Chem. Eng. J. 361 (2019) 885–896.

[81] Z. Shayegan, C.-S. Lee, F. Haghighat, TiO_2 photocatalyst for removal of volatile organic compounds in gas phase – a review, Chem. Eng. J. 334 (2018) 2408–2439.

[82] S. Zhang, C. Ye, H. Lin, L. Lv, X. Yu, UV disinfection induces a VBNC state in Escherichia coli and Pseudomonas aeruginosa, Environ. Sci. Technol. 49 (2015) 1721-1728.

[83] S. Chen, X. Li, Y. Wang, J. Zeng, C. Ye, X. Li, L. Guo, S. Zhang, X. Yu, Induction of Escherichia coli into a VBNC state through chlorination/chloramination and differences in characteristics of the bacterium between states, Water Res. 142 (2018) 279–288.

[84] T. Vladkova, O. Angelov, D. Stoyanova, D. Gospodinova, L. Gomes, A. Soares, F. Mergulhao, I. Ivanova, Magnetron co-sputtered TiO_2/SiO_2/Ag nanocomposite thin coatings inhibiting bacterial adhesion and biofilm formation, Surf. Coat. Technol. 384 (2020), 125322.

[85] N. Hao, Y. Nie, J.X.J. Zhang, Biomimetic hierarchical walnut kernel-like and erythrocyte-like mesoporous silica nanomaterials: controllable synthesis and versatile applications, Microporous Mesoporous Mater. 261 (2018) 144–149.

[86] M.K. Kaygusuz, M. Meyer, A. Aslan, The effect of TiO_2-SiO_2 nanocomposite on the performance characteristics of leather, Mater. Res. 20 (2017) 1103-1110.

[87] J.-M. Zhang, J. Liu, K. Wang, X. Zhang, T. Zhao, H.-M. Luo, Observations of bacterial biofilm on ureteral stent and studies on the distribution of pathogenic bacteria and drug resistance, Urol. Int. 101 (2018) 320–326.

[88] Y. Ohko, Y. Utsumi, C. Niwa, T. Tatsuma, K. Kobayakawa, Y. Satoh, Y. Kubota, A. Fujishima, Self-sterilizing and self-cleaning of silicone catheters coated with TiO_2 photocatalyst thin films: a preclinical work, J. Biomed. Mater. Res. 58 (2001) 97–101.

[89] O.M. Bondarenko, M. Sihtmäe, J. Kuzmičiova, L. Ragelienė, A. Kahru, R. Daugelavičius, Plasma membrane is the target of rapid antibacterial action of silver nanoparticles in Escherichia coli and Pseudomonas aeruginosa, Int. J. Nanomed. 13 (2018) 6779.

[90] A. Ahmad, Y. Wei, F. Syed, K. Tahir, A.U. Rehman, A. Khan, S. Ullah, Q. Yuan, The effects of bacteria-nanoparticles interface on the antibacterial activity of green synthesized silver nanoparticles, Microb. Pathog. 102 (2017) 133–142.

[91] D.A. Ashmore, A. Chaudhari, B. Barlow, B. Barlow, T. Harper, K. Vig, M. Miller, S. Singh, E. Nelson, S. Pillai, Evaluation of E. coli inhibition by plain and polymer-coated silver nanoparticles, Revista do Instituto de Medicina Tropical de São Paulo 60 (2018) e18.

[92] N.A. Mazurkova, Y.E. Spitsyna, N.V. Shikina, Z.R. Ismagilov, S.N. Zagrebel'nyi, E. I. Ryabchikova, Interaction of titanium dioxide nanoparticles with influenza virus, Nanotechnol. Russ. 5 (2010) 417-420.

[93] R. Nakano, H. Ishiguro, Y. Yao, J. Kajioka, A. Fujishima, K. Sunada, M. Minoshima, K. Hashimoto, Y. Kubota, Photocatalytic inactivation of influenza virus by titanium dioxide thin film, Photochem. Photobiol. Sci. 11 (2012) 1293.

[94] K. Shiraki, H. Yamada, Y. Yoshida, A. Ohno, T. Watanabe, T. Watanabe, H. Watanabe, H. Watanabe, M. Yamaguchi, F. Tokuoka, S. Hashimoto, M. Kawamura, N. Adachi, Improved photocatalytic air cleaner with decomposition of aldehyde and aerosol-associated influenza virus infectivity in indoor air, Aerosol Air Qual. Res. 17 (2017) 2901–2912.

[95] N. Doss, G. Carré, V. Keller, P. André, N. Keller, Photocatalytic decontamination of airborne T2 bacteriophage viruses in a small-size TiO_2/β-SiC alveolar foam LED reactor, Water, Air, Soil Pollut. 229 (2018) 29.

[96] X. Zheng, Z.-peng. Shen, C. Cheng, L. Shi, R. Cheng, D.-hai. Yuan, Photocatalytic disinfection performance in virus and virus/bacteria system by Cu-TiO_2 nanofibers under visible light, Environ. Pollut. 237 (2018) 452–459.

[97] A. Habibi-Yangjeh, S. Asadzadeh-Khaneghah, S. Feizpoor, A. Rouhi, Review on heterogeneous photocatalytic disinfection of waterborne, airborne, and foodborne viruses: can we win against pathogenic viruses? J. Colloid Interface Sci. 580 (2020) 503–514.

[98] M. Kaur, K. Singh, Review on titanium and titanium based alloys as biomaterials for orthopaedic applications, Mater. Sci. Eng., C 102 (2019) 844–862.

[99] H. Attar, S. Ehtemam-Haghighi, N. Soro, D. Kent, M.S. Dargusch, Additive manufacturing of low-cost porous titanium-based composites for biomedical applications: advantages, challenges and opinion for future development, J. Alloys Compd. 827 (2020), 154263.

[100] M. Mansoorianfar, A. Khataee, Z. Riahi, K. Shahin, M. Asadnia, A. Razmjou, A. Hojjati-Najafabadi, C. Mei, Y. Orooji, D. Li, Scalable fabrication of tunable titanium nanotubes via sonoelectrochemical process for biomedical applications, Ultrason. Sonochem. 64 (2020), 104783.

[101] J. Ni, H. Ling, S. Zhang, Z. Wang, Z. Peng, C. Benyshek, R. Zan, A. Miri, Z. Li, X. Zhang, Three-dimensional printing of metals for biomedical applications, Mater. Today Bio 3 (2019), 100024.

[102] Z. Lei, H. Zhang, E. Zhang, J. You, X. Ma, X. Bai, Antibacterial activities and biocompatibilities of Ti-Ag alloys prepared by spark plasma sintering and acid etching, Mater. Sci. Eng., C 92 (2018) 121–131.

[103] L.H. Barros, T.A. Barbosa, J. Esteves, M. Abreu, D. Soares, R. Sousa, Early Debridement, antibiotics and implant retention (DAIR) in patients with suspected acute infection after hip or knee arthroplasty-safe, effective and without negative functional impact, J. Bone Joint Infect. 4 (2019) 300-305.

[104] L. Tan, J. Fu, F. Feng, X. Liu, Z. Cui, B. Li, Y. Han, Y. Zheng, K.W.K. Yeung, Z. Li, Engineered probiotics biofilm enhances osseointegration via immunoregulation and anti-infection, Sci. Adv. 6 (2020) eaba5723.

[105] H. Koo, R.N. Allan, R.P. Howlin, P. Stoodley, L. Hall-Stoodley, Targeting microbial biofilms: current and prospective therapeutic strategies, Nat. Rev. Microbiol. 15 (2017) 740–755.

[106] S. Yu, D. Guo, J. Han, L. Sun, H. Zhu, Z. Yu, M. Dargusch, G. Wang, Enhancing antibacterial performance and biocompatibility of pure titanium by a two-step electrochemical surface coating, ACS Appl. Mater. Interfaces 12 (2020) 44433–44446.

[107] X. Zhang, Y. Lv, S. Fu, Y. Wu, X. Lu, L. Yang, H. Liu, Z. Dong, Synthesis, microstructure, anti-corrosion property and biological performances of Mn-incorporated Ca-P/TiO_2 composite coating fabricated via micro-arc oxidation, Mater. Sci. Eng., C 117 (2020), 111321.

[108] L. Yu, Y. Tian, Y. Qiao, X. Liu, Mn-containing titanium surface with favorable osteogenic and antimicrobial functions synthesized by PIII&D, Colloids Surf. B 152 (2017) 376–384.

[109] Y. Huang, H. Qiao, X. Nian, X. Zhang, X. Zhang, G. Song, Z. Xu, H. Zhang, S. Han, Improving the bioactivity and corrosion resistance properties of electrodeposited hydroxyapatite coating by dual doping of bivalent strontium and manganese ion, Surf. Coat. Technol. 291 (2016) 205–215.

[110] L. Yu, S. Qian, Y. Qiao, X. Liu, Multifunctional Mn-containing Titania coatings with enhanced corrosion resistance, osteogenesis and antibacterial activity, J. Mater. Chem. B 2 (2014) 5397.

[111] Y.-T. Liu, K.-C. Kung, T.-M. Lee, T.-S. Lui, Enhancing biological properties of porous coatings through the incorporation of manganese, J. Alloy. Compd. 581 (2013) 459–467.

[112] J.G. Souza, M. Bertolini, R.C. Costa, J.M. Cordeiro, B.E. Nagay, A.B. de Almeida, B. Retamal-Valdes, F.H. Nociti, M. Feres, E.C. Rangel, Targeting pathogenic biofilms: newly developed superhydrophobic coating favors a host-compatible microbial profile on the titanium surface, ACS Appl. Mater. Interfaces 12 (2020) 10118–10129.

[113] S.E. Cross, J. Kreth, L. Zhu, R. Sullivan, W. Shi, F. Qi, J.K. Gimzewski, Nanomechanical properties of glucans and associated cell-surface adhesion of Streptococcus mutans probed by atomic force microscopy under in situ conditions, Microbiology 153 (2007) 3124-3132.

[114] M.J. Mestnik, M. Feres, L.C. Figueiredo, P.M. Duarte, E.A.G. Lira, M. Faveri, Short-term benefits of the adjunctive use of metronidazole plus amoxicillin in the microbial profile and in the clinical parameters of subjects with generalized aggressive periodontitis, Journal of clinical periodontology 37 (2010) 353-365.

[115] G.R. Persson, E. Samuelsson, C. Lindahl, S. Renvert, Mechanical non-surgical treatment of peri-implantitis: a single-blinded randomized longitudinal clinical study. II. Microbiological results, J. Clin. Periodontol. 37 (2010) 563–573.

[116] R. Wang, M. Shi, F. Xu, Y. Qiu, P. Zhang, K. Shen, Q. Zhao, J. Yu, Y. Zhang, Graphdiyne-modified TiO_2 nanofibers with osteoinductive and enhanced photocatalytic antibacterial activities to prevent implant infection, Nat. Commun. 11 (2020) 4465.

[117] Y. Zhang, W. Liu, Y. Li, Y.-W. Yang, A. Dong, Y. Li, 2D graphdiyne oxide serves as a superior new generation of antibacterial agents, iScience 19 (2019) 662–675.

[118] J. Xie, N. Wang, X. Dong, C. Wang, Z. Du, L. Mei, Y. Yong, C. Huang, Y. Li, Z. Gu, Y. Zhao, Graphdiyne nanoparticles with high free radical scavenging activity for radiation protection, ACS Appl. Mater. Interfaces 11 (2019) 2579–2590.

[119] L. Dieltjens, K. Appermans, M. Lissens, B. Lories, W. Kim, E.V. Van der Eycken, K. R. Foster, H.P. Steenackers, Inhibiting bacterial cooperation is an evolutionarily robust anti-biofilm strategy, Nat. Commun. 11 (2020) 107.

[120] A. Kramer, I. Schwebke, G. Kampf, How long do nosocomial pathogens persist on inanimate surfaces? A systematic review, BMC Infect. Dis. 6 (2006) 130.

[121] S. Riddell, S. Goldie, A. Hill, D. Eagles, T.W. Drew, The effect of temperature on persistence of SARS-CoV-2 on common surfaces, Virol. J. 17 (2020) 145.

[122] G. Humphreys, F. Fleck, United Nations meeting on antimicrobial resistance, World Health Organization, Bull. World Health Organ. 94 (2016) 638.

[123] W.H. Organization, Fact sheets on sustainable development goals: health targets. Antimicrobial Resistance 2017.

[124] M. Nicola, Z. Alsafi, C. Sohrabi, A. Kerwan, A. Al-Jabir, C. Iosifidis, M. Agha, R. Agha, The socio-economic implications of the coronavirus pandemic (COVID-19): a review, Int. J. Surg. 78 (2020) 185–193.

[125] A. Mills, G. Hill, S. Bhopal, I.P. Parkin, S.A. O'Neill, Thick titanium dioxide films for semiconductor photocatalysis, J. Photochem. Photobiol., A 160 (2003) 185–194.

[126] F.S. Froes, Titanium for medical and dental applications—An introduction, Titanium in Medical and Dental Applications, Woodhead Publishing Series in Biomaterials (2018) 3-21.

[127] V. Alt, Antimicrobial coated implants in trauma and orthopaedics–a clinical review and risk-benefit analysis, Injury 48 (2017) 599–607.

[128] G. Asensio, B. Vázquez-Lasa, L. Rojo, Achievements in the topographic design of commercial titanium dental implants: towards anti-peri-implantitis surfaces, J. Clin. Med. 8 (2019) 1982.

[129] R. Ragadhita, A.B.D. Nandiyanto, A.C. Maulana, R. Oktiani, A. Sukmafitri, A. Machmud, E. Surachman, Techno-economic analysis for the production of titanium dioxide nanoparticle produced by liquid-phase synthesis method, J. Eng. Sci. Technol. 14 (2019) 1639–1652.

[130] H. Babaizadeh, M. Hassan, Life cycle assessment of nano-sized titanium dioxide coating on residential windows, Constr. Build. Mater. 40 (2013) 314–321.

[131] K. Ettrup, A. Kounina, S.F. Hansen, J.A. Meesters, E.B. Vea, A. Laurent, Development of comparative toxicity potentials of TiO_2 nanoparticles for use in life cycle assessment, Environ. Sci. Technol. 51 (2017) 4027-4037.

[132] C. Moro, V. Francioso, M. Schrager, M. Velay-Lizancos, TiO_2 nanoparticles influence on the environmental performance of natural and recycled mortars: a life cycle assessment, Environ. Impact Assess. Rev. 84 (2020) 106430.

[133] M. Qadir, J. Lin, A. Biesiekierski, Y. Li, C. Wen, Effect of Anodized TiO_2–Nb_2O_5–ZrO_2 Nanotubes with Different Nanoscale Dimensions on the Biocompatibility of a Ti35Zr28Nb Alloy, ACS Appl. Mater. Interfaces 12 (2020) 6776-6787.

[134] N. Farajpour, R. Deivanayagam, A. Phakatkar, S. Narayanan, R. Shahbazian-Yassar, T. Shokuhfar, A novel antimicrobial electrochemical glucose biosensor based on silver–Prussian blue-modified TiO_2 nanotube arrays, Med. Devices Sens. 3 (2020) e10061.

[135] N.P. Shetti, S.D. Bukkitgar, K.R. Reddy, C.V. Reddy, T.M. Aminabhavi, Nanostructured titanium oxide hybrids-based electrochemical biosensors for healthcare applications, Colloids Surf. B 178 (2019) 385–394.

[136] N.P. Shetti, D.S. Nayak, S.J. Malode, R.R. Kakarla, S.S. Shukla, T.M. Aminabhavi, Sensors based on ruthenium-doped TiO_2 nanoparticles loaded into multi-walled carbon nanotubes for the detection of flufenamic acid and mefenamic acid, Anal. Chim. Acta 1051 (2019) 58–72.

[137] H. Salazar, P. Martins, B. Santos, M. Fernandes, A. Reizabal, V. Sebastián, G. Botelho, C.J. Tavares, J.L. Vilas-Vilela, S. Lanceros-Mendez, Photocatalytic and antimicrobial multifunctional nanocomposite membranes for emerging pollutants water treatment applications, Chemosphere 250 (2020), 126299.

[138] S. Hosseinzadeh, R. Partovi, F. Talebi, A. Babaei, Chitosan/TiO_2 nanoparticle/Cymbopogon citratus essential oil film as food packaging material: Physico-mechanical properties and its effects on microbial, chemical, and organoleptic quality of minced meat during refrigeration, J. Food Process. Preserv. (2020) e14536.

[139] F. Xiao, C. Zong, W. Wang, X.-zhu. Liu, A. Osaka, X.-chun. Ma, Low-temperature fabrication of Titania layer on 3D-printed 316L stainless steel for enhancing biocompatibility, Surf. Coat. Technol. 367 (2019) 91–99.

[140] S. Sütterlin, M. Dahlö, C. Tellgren-Roth, W. Schaal, Å. Melhus, High frequency of silver resistance genes in invasive isolates of Enterobacter and Klebsiella species, J. Hosp. Infect. 96 (2017) 256–261.
[141] D.L. Monnet, S. Harbarth, Will coronavirus disease (COVID-19) have an impact on antimicrobial resistance? Eurosurveillance 25 (2020) 2001886.
[142] A.K. Murray, The Novel Coronavirus COVID-19 Outbreak: Global Implications for Antimicrobial Resistance, Front. Microbiol. 11 (2020).
[143] J.A. Bengoechea, C.G. Bamford, SARS-CoV-2, bacterial co-infections, and AMR: the deadly trio in COVID-19? EMBO Mol. Med. 12 (2020), e12560.
[144] S. Kampmeier, H. Tönnies, C.L. Correa-Martinez, A. Mellmann, V. Schwierzeck, A nosocomial cluster of vancomycin resistant enterococci among COVID-19 patients in an intensive care unit, Antimicrob. Resist. Infect. Control 9 (2020) 154.
[145] P. Nori, W. Szymczak, Y. Puius, A. Sharma, K. Cowman, P. Gialanella, Z. Fleischner, M. Corpuz, J. Torres-Isasiga, R. Bartash, Emerging co-pathogens: New Delhi metallo-beta-lactamase producing enterobacterales infections in New York City COVID-19 patients, Int. J. Antimicrob. Agents 56 (2020), 106179.
[146] B. Tiri, E. Sensi, V. Marsiliani, M. Cantarini, G. Priante, C. Vernelli, L.A. Martella, M. Costantini, A. Mariottini, P. Andreani, Antimicrobial stewardship program, COVID-19, and infection control: spread of carbapenem-resistant klebsiella pneumoniae colonization in ICU COVID-19 patients. What Did Not Work? J Clin. Med. 9 (2020) 2744.
[147] A. Katz, A. McDonagh, L. Tijing, H.K. Shon, Fouling and inactivation of titanium dioxide-based photocatalytic systems, Crit. Rev. Environ. Sci. Technol. 45 (2015) 1880–1915.
[148] G. Huang, D. Xia, T. An, T.W. Ng, H.Y. Yip, G. Li, H. Zhao, P.K. Wong, M. Kivisaar, Dual roles of capsular extracellular polymeric substances in photocatalytic inactivation of Escherichia coli: comparison of E. coli BW25113 and isogenic mutants, Appl. Environ. Microbiol. 81 (2015) 5174–5183.
[149] K.T. Kim, M.Y. Eo, T.T.H. Nguyen, S.M. Kim, General review of titanium toxicity, Int. J. Implant Dent. 5 (2019) 10.
[150] A. Markowska-Szczupak, M. Endo-Kimura, O. Paszkiewicz, E. Kowalska, Are Titania photocatalysts and titanium implants safe? Review on the toxicity of titanium compounds, Nanomaterials 10 (2020) 2065.